JCI The Journal of Clinical Investigation

Neural crest–derived SEMA3C activates endothelial NRP1 for cardiac outflow tract septation

Alice Plein, … , Peter J. Scambler, Christiana Ruhrberg

J Clin Invest. 2015;125(7):2661-2676. https://doi.org/10.1172/JCI79668.

Research Article **Vascular biology**

In mammals, the outflow tract (OFT) of the developing heart septates into the base of the pulmonary artery and aorta to guide deoxygenated right ventricular blood into the lungs and oxygenated left ventricular blood into the systemic circulation. Accordingly, defective OFT septation is a life-threatening condition that can occur in both syndromic and nonsyndromic congenital heart disease. Even though studies of genetic mouse models have previously revealed a requirement for VEGF-A, the class 3 semaphorin SEMA3C, and their shared receptor neuropilin 1 (NRP1) in OFT development, the precise mechanism by which these proteins orchestrate OFT septation is not yet understood. Here, we have analyzed a complementary set of ligand-specific and tissue-specific mouse mutants to show that neural crest–derived SEMA3C activates NRP1 in the OFT endothelium. Explant assays combined with gene-expression studies and lineage tracing further demonstrated that this signaling pathway promotes an endothelial-to-mesenchymal transition that supplies cells to the endocardial cushions and repositions cardiac neural crest cells (NCCs) within the OFT, 2 processes that are essential for septal bridge formation. These findings elucidate a mechanism by which NCCs cooperate with endothelial cells in the developing OFT to enable the postnatal separation of the pulmonary and systemic circulation.

Neural crest–derived SEMA3C activates endothelial NRP1 for cardiac outflow tract septation

Alice Plein,[1] Amélie Calmont,[2] Alessandro Fantin,[1] Laura Denti,[1] Naomi A. Anderson,[2] Peter J. Scambler,[2] and Christiana Ruhrberg[1]

[1]UCL Institute of Ophthalmology and [2]UCL Institute of Child Health, University College London, London, United Kingdom.

In mammals, the outflow tract (OFT) of the developing heart septates into the base of the pulmonary artery and aorta to guide deoxygenated right ventricular blood into the lungs and oxygenated left ventricular blood into the systemic circulation. Accordingly, defective OFT septation is a life-threatening condition that can occur in both syndromic and nonsyndromic congenital heart disease. Even though studies of genetic mouse models have previously revealed a requirement for VEGF-A, the class 3 semaphorin SEMA3C, and their shared receptor neuropilin 1 (NRP1) in OFT development, the precise mechanism by which these proteins orchestrate OFT septation is not yet understood. Here, we have analyzed a complementary set of ligand-specific and tissue-specific mouse mutants to show that neural crest–derived SEMA3C activates NRP1 in the OFT endothelium. Explant assays combined with gene-expression studies and lineage tracing further demonstrated that this signaling pathway promotes an endothelial-to-mesenchymal transition that supplies cells to the endocardial cushions and repositions cardiac neural crest cells (NCCs) within the OFT, 2 processes that are essential for septal bridge formation. These findings elucidate a mechanism by which NCCs cooperate with endothelial cells in the developing OFT to enable the postnatal separation of the pulmonary and systemic circulation.

Introduction

Congenital heart defects are a leading cause of perinatal mortality and morbidity, affecting 1% of all live births in the Western world (1). A common arterial trunk (CAT, also known as persistent truncus arteriosus) is a rare defect caused by faulty remodeling of the heart outflow tract (OFT) during embryogenesis. The OFT is a transient embryonic structure at the arterial pole of the heart that initially functions as a conduit for blood flowing from the right ventricle into the aortic sac. Subsequently, the OFT wall rotates and septates to generate the base of the ascending aorta and pulmonary trunk, which enables the separation of the arterial and venous circulation. A failure of OFT septation during embryogenesis therefore results in inappropriate mixing of oxygenated and deoxygenated blood at birth and has an unfavorable clinical prognosis (2).

Initially, the OFT comprises a solitary tube filled with an acellular cardiac jelly of extracellular matrix components that is gradually colonized by cells from several distinct sources to form the endocardial cushions as a prerequisite for septation (3, 4). Cushion formation and septation rely on the interaction of 3 distinct cell types, cardiac neural crest cells (NCCs), second heart field–derived (SHF-derived) cells, and endothelial cells (ECs). The immigration of cardiac NCCs into the OFT correlates with an endothelial-to-mesenchymal (endoMT) transition of OFT endothelium into mesenchymal cells that colonize the cushions (5). Once the endocardial cushions have sufficiently expanded, the OFT endothelium fuses, starting in the distal and progressing to the proximal part of the tract, and a septal bridge is formed. SHF-derived smooth muscle cells (SMCs) from the OFT wall and myocardium enter the emerging septum to complete the septation process through myocardialization (6, 7). Eventually, the leading edge of the muscular septum attaches to the interventricular septum, thus fusing the base of the aorta and the base of the pulmonary artery to the ventricles.

The molecular mechanisms by which cardiac NCCs, SHF-derived cells, and ECs cooperate during OFT septation are partially understood. Two signaling cues essential for OFT septation are the class 3 semaphorin SEMA3C and the vascular endothelial growth factor VEGF-A. Thus, lack of OFT septation is seen in *Sema3c*-null mice (8) and *Vegfa*$^{120/120}$ mice expressing the VEGF120 isoform of VEGF-A at the expense of the larger, heparin/neuropilin-binding isoforms VEGF165 and VEGF188 (9). However, the precise cellular mechanisms by which these ligands promote OFT remodeling are unknown.

Neuropilin 1 (NRP1) is a transmembrane receptor for both SEMA3C and VEGF165 (10). Consistent with an essential role for NRP1 in OFT remodeling, *Nrp1*-null mice have CAT (11). The finding that endothelial NRP1 is required for OFT septation in the mouse has been interpreted as evidence that it functions as a VEGF165 receptor during endothelial remodeling in the OFT (12, 13). Yet it has not been demonstrated that VEGF-A binding to NRP1 is essential for this process. Additionally, it has been suggested that NRP1 serves as a semaphorin receptor in cardiac NCCs, where it is partially redundant with its homolog NRP2 (13, 14). To convey semaphorin signals in cardiac NCCs, NRPs are thought to form a complex with a plexin coreceptor termed PLXNA2, which is expressed in cardiac NCCs (15). However, a role for

Authorship note: Alice Plein and Amélie Calmont contributed equally to this work.
Conflict of interest: The authors have declared that no conflict of interest exists.
Submitted: November 7, 2014; **Accepted:** April 30, 2015.
Reference information: *J Clin Invest*. 2015;125(7):2661–2676. doi:10.1172/JCI79668.

NRPs in cardiac NCCs has never been demonstrated directly for mammalian OFT remodeling.

Here, we have investigated OFT development in tissue-specific knockout mice to compare the requirement of NRP1 in OFT endothelium versus cardiac NCCs. We have also examined NRP1 knockin mice with mutations that selectively target VEGF-A versus SEMA3 binding to distinguish the relative contribution of both ligands to NRP1 signaling during OFT septation. This analysis revealed that NRP1 expression by cardiac NCCs and VEGF binding to NRP1 are both dispensable for OFT remodeling, even when NRP2 is additionally ablated. Instead, we found that loss of endothelial NRP1 was sufficient to recapitulate the OFT phenotype of *Nrp1*-null mice because NRP1 served as a receptor for SEMA3C in ECs. We further show that cardiac NCCs, contrary to prior hypotheses, do not respond to SEMA3C, but instead provide an essential source of SEMA3C. Thus, NCC-derived SEMA3C promotes endoMT via NRP1 and, indirectly, cardiac NCC relocalization within the OFT, 2 prerequisites for septal bridge formation in the proximal OFT. These findings identify a mechanism by which cardiac NCCs communicate with ECs to orchestrate OFT septation and therefore enable the separation of the arterial and pulmonary circulation for life after birth.

Results

Multiple roles for NRP1 during OFT remodeling. Ink injections into whole-mount hearts were previously used to demonstrate a lack of OFT septation in *Nrp1*-null mutants (11). Because this technique does not reveal which specific aspects of OFT septation are defective, we devised a method that distinguishes several different processes critical for OFT septation. Thus, we immunolabeled serial sections through OFTs at E12.5 with the SMC marker smooth muscle α actin (SMA) and the vascular endothelial marker PECAM (Figure 1, A and B) to assess endocardial cushion swelling, endothelial fusion, and the invasion of smooth muscle and myocardial cells into the septal bridge (Figure 1B, top row). This method showed that all *Nrp1*-null mutants lacked septation throughout the entire OFT, including its proximal and distal parts (Figure 1B, middle row), and revealed that the endocardial cushions of mutants were abnormally oriented relative to the heart. In addition, mutant OFTs contained atypical associations between the endocardium and myocardium, causing cushion disorganization, similar to that seen in endothelial *Nrp1*-null mutants (12). *Nrp1*-null mutants also lacked myocardialization of the septal bridge (Figure 1B), with SMA-positive cells appearing to stall within the endocardial cushions in peripheral positions (Figure 1, B and C). In contrast, mice lacking NRP2 displayed normal OFT septation, OFT rotation, and myocardialization of the septal bridge (Figure 1B, bottom row).

Expression pattern of NRP1 during OFT remodeling. To define the NRP1 expression pattern during OFT remodeling, we immunolabeled serial sections through an E12.5 WT OFT with a validated antibody for NRP1 (16) together with SMA and the vascular endothelial marker isolectin B4 (IB4) (Figure 2, A and B). This analysis demonstrated that NRP1 is expressed weakly on migrating SMA-positive cells and strongly on IB4-positive ECs (Figure 2, A and B). In contrast, there was no obvious NRP1 expression within the region occupied by the postmigratory cardiac NCC population (Figure 2A).

Cardiac NCCs and endothelium-derived cells give rise to distinct parts of the OFT. To show that the *Wnt1-Cre* and *Tie2-Cre* transgenes selectively target NRP1 in cardiac NCCs versus ECs and to determine the relative position of their progeny via lineage tracing, we immunolabeled serial sections of E12.5 *Wnt1-Cre Rosa*^{Yfp} and *Tie2-Cre Rosa*^{Yfp} OFTs for YFP. As expected, *Tie2-Cre* targeted the endothelium, whereas *Wnt1-Cre* did not (Figure 3A). Instead, *Wnt1-Cre*–targeted cardiac NCCs contributed to the semilunar valve leaflets and septal bridge (Figure 3A). In the *Tie2-Cre* lineage–traced OFT, many individual YFP-positive cells were present in the endocardial cushions (Figure 3A), consistent with the previously described contribution of endoMT-derived cells to the endocardial cushions (17–19). *Tie2-Cre* lineage–traced cells also contributed to the semilunar valves (Figure 3A). This analysis therefore confirmed the distinct contributions of EC- and cardiac NCC–derived lineages to the OFT.

NCC-derived NRP1 is not required for OFT septation in the mouse. Because a role for NRP1 in cardiac NCC migration had previously been reported in chick (14), we investigated whether cardiac NCC–derived NRP1 is required for OFT septation in mice by comparing immunolabeled serial sections through the E12.5 OFTs of *Wnt1-Cre Nrp1*$^{fl/fl}$ mutants and controls. Efficient targeting of NRP1 in the NCC lineage was previously demonstrated by similar defects in the NCC-derived sympathetic nervous systems of *Wnt1-Cre Nrp1*$^{fl/fl}$ mutants and full *Nrp1* knockouts (20). However, and in contrast with *Nrp1*$^{-/-}$ mice, the OFTs of *Wnt1-Cre Nrp1*$^{fl/fl}$ mutants were septated normally (Figure 3B, top panels). To address whether NRP2 compensated for the lack of NRP1 in cardiac NCCs, as previously proposed (13, 14), we crossed *Wnt1-Cre Nrp1*$^{fl/fl}$ mutants onto an *Nrp2*-null background. However, compound mutants also showed normal OFT septation, rotation, and myocardialization (Figure 3B, middle panels). Contrary to prior hypotheses, NRP1 and NRP2 expression by cardiac NCCs is therefore not required for OFT remodeling.

Endothelial NRP1 is essential for OFT septation in the mouse. Ink injections previously demonstrated that mice lacking endothelial NRP1 (*Tie2-Cre Nrp1*$^{fl/-}$) have defective OFT septation (12, 13). Using immunolabeling of serial sections, we confirmed that *Tie2-Cre Nrp1*$^{fl/-}$ mutants had OFT defects similar to full NRP1 knockouts (Figure 3B, bottom panels). In particular, our method demonstrated septation defects in both the proximal and distal part of mutant OFTs as well as abnormal associations between the endocardium and myocardium (Figure 3B, bottom panels). Furthermore, *Tie2-Cre Nrp1*$^{fl/-}$ OFTs showed failed rotation and impaired septal bridge myocardialization (Figure 3B, bottom panels). Taken together with the analysis of NCC-specific *Nrp1* mutants, these observations suggest that all essential NRP1 signaling during OFT remodeling takes place in the vascular endothelium.

VEGF-A signaling through NRPs is dispensable for OFT septation. Prior studies observed CAT in *Vegfa*$^{120/120}$ mice, which express VEGF120 at the expense of the longer, heparin/NRP-binding isoforms of VEGF-A (9). Together with the finding that mice lacking endothelial NRP1 display defective OFT septation, the phenotype of *Vegfa*$^{120/120}$ mice was previously interpreted as evidence for an essential role of VEGF-A signaling through NRP1 in OFT remodeling (13). However, neither prior study was able to directly address the role of VEGF-A as a NRP1 ligand in OFT

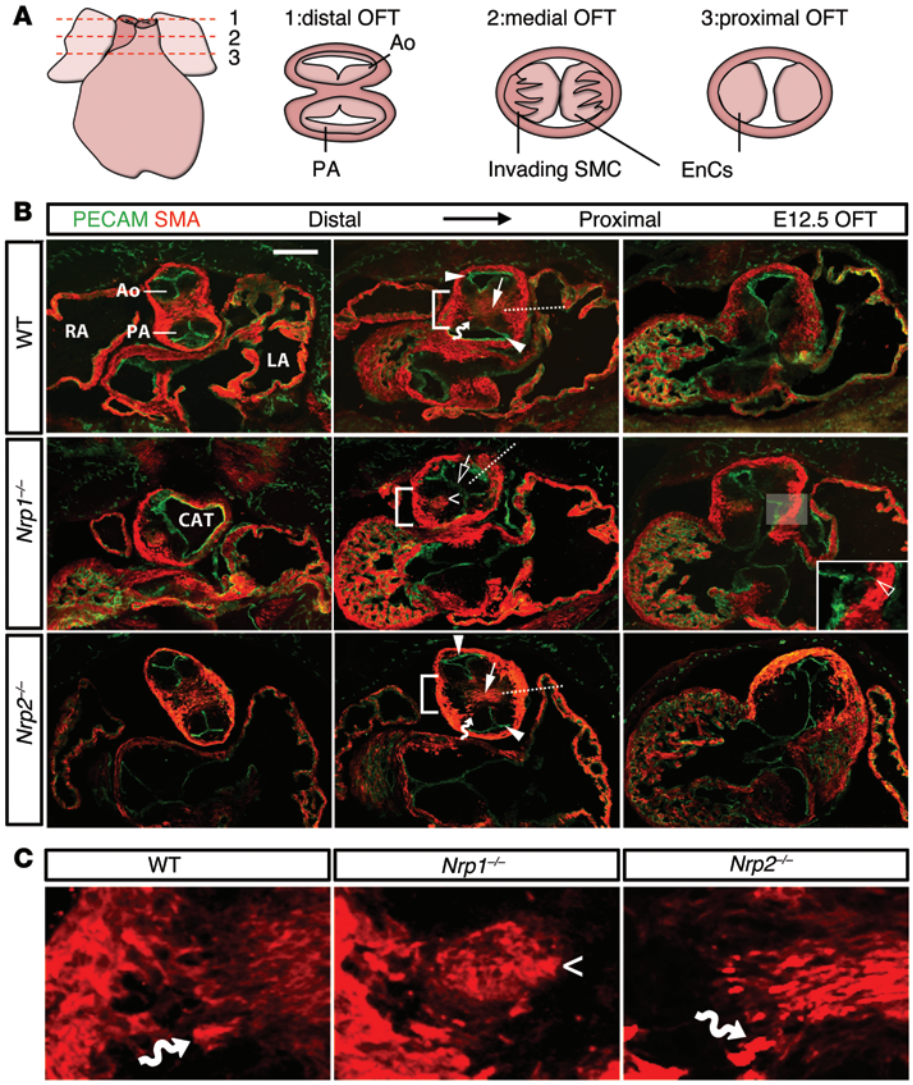

Figure 1. NRP1, not NRP2, enables endocardial cushion organization, endothelial fusion, OFT rotation, and septal bridge myocardialization in the remodeling OFT. (**A**) Schematic representation of E12.5 mouse OFT at distal (no. 1), medial (no. 2), and proximal (no. 3) positions relative to the heart. (**B** and **C**) Serial sections of WT, *Nrp1*$^{-/-}$ (n = 6), and *Nrp2*$^{-/-}$ (n = 3) E12.5 OFTs at corresponding proximal, medial, and distal levels were immunolabeled for the endothelial marker PECAM and the SMC and myocyte marker SMA. High magnification of areas indicated by squared brackets in **B** is shown in **C** as single SMA channels. Solid arrowheads indicate endothelium of the aorta and pulmonary artery; solid arrows indicate septal bridge myocardialization; and open arrows indicate the absence of septal bridge formation. Wavy arrows highlight migrating SMA-positive cells and angles stalled SMA-positive cells. Dotted lines indicate the axis of septal bridge formation, and the open arrowhead indicates an atypical association between OFT endothelium and myocardium. Ao, aorta; PA, pulmonary artery; EnCs, endocardial cushions; LA, left atrium; RA, right atrium. Scale bar: 200 μm (**B**).

development because a mouse mutant defective in VEGF-A binding to NRP1 was not available at the time. Moreover, the *Vegfa* expression pattern had not been analyzed to determine whether NCCs provide an important source of this growth factor for OFT remodeling. We therefore determined the *Vegfa* expression pattern and analyzed the OFTs of mice lacking VEGF-A expression in NCCs or VEGF-A binding to NRP1.

Using the established *Vegfa* expression reporter *Vegfa*^{Lacz} (21), we observed weak *Vegfa* expression by the OFT endothelium and strong expression by the SHF-derived myocardial OFT cuff at E12.5 (Figure 4A). In contrast, *Vegfa* expression appeared absent from the area occupied by cardiac NCCs (Figure 4A). To confirm that cardiac NCCs are not a critical source of VEGF-A for OFT septation, we introduced *Wnt1-Cre* into mice with conditional *Vegfa*-null alleles (*Vegfa*$^{fl/fl}$) (22). In agreement with the lack of obvious *Vegfa* expression in OFT NCCs, *Wnt1-Cre*;*Vegfa*$^{fl/fl}$ OFTs had normal septation (Figure 4B). These findings demonstrate that cardiac NCCs do not express VEGF-A to promote OFT septation.

To determine whether NRP1 serves as a VEGF-A receptor in OFT development, we used mice with a knockin mutation that impairs VEGF-A binding to NRP1 (23), designated here as *Nrp1*$^{Vegfa/Vegfa}$ mutants. Immunolabeling of serial sections for PECAM and SMA revealed that OFT septation, rotation, and myocardialization were normal in *Nrp1*$^{Vegfa/Vegfa}$ mutants, even on an *Nrp2*-null background (Figure 4C), excluding compensation by NRP2. Thus, contrary to prior hypotheses, endothelial NRP1 does not act as a VEGF-A receptor during OFT septation.

SEMA3C is expressed by myocardial cuff cells and cardiac NCCs in the septal bridge. Even though SEMA3C is essential for OFT septation (8, 24), its precise role in this process has not been determined to date. In agreement with prior findings (8, 25), we observed *Sema3c* expression in the myocardial cuff that surrounds the aortic segment of the OFT from E10.5 onwards (Figure 5A). In addition, *Sema3c* was expressed in the area where cardiac NCCs were located from E11.5 onwards (Figure 5A). Several prior studies interpreted this expression pattern as an indication that SEMA3C attracts cardiac NCCs into the OFT (8, 14). In contrast, other studies have speculated that *Sema3c* may also be expressed by cardiac NCCs themselves (25, 26). To resolve this controversy, we performed *Sema3c* ISH on *Wnt1-Cre Rosa*^{Yfp} OFTs and found that *Sema3c* was expressed in a subpopulation of the cardiac NCC lineage (Figure 5B). Double immunolabeling of sections from *Wnt1-Cre Rosa*^{Yfp}

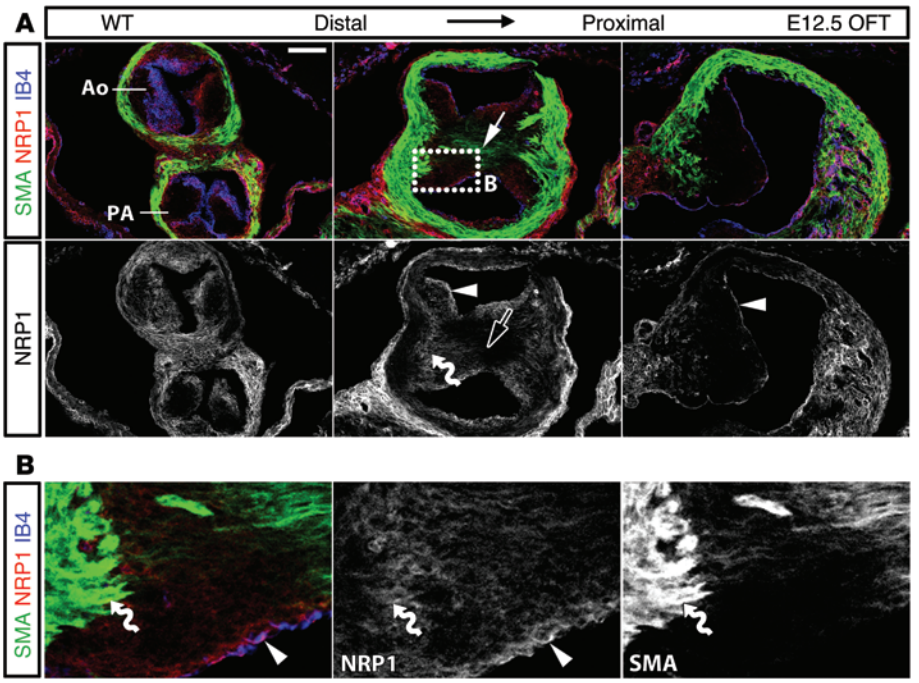

Figure 2. NRP1 expression in ECs, but not the septal bridge of the remodeling OFT. (**A** and **B**) Serial E12.5 OFT sections at distal, medial, and proximal positions were immunolabeled for NRP1, SMA, and the vascular endothelial marker IB4. High magnification of the boxed area indicated in **A** is shown in **B**. Arrowheads indicate strong NRP1 expression on endothelium and wavy arrows indicate weak expression on SMA-positive migrating cells. The solid arrow indicates SMA staining in the septal bridge, while the open arrow highlights lack of NRP1 expression in the septal bridge. Scale bar: 100 μm (**A**).

embryos for YFP and PLXNA2, an established marker for a subset of cardiac NCCs in the OFT (15), further showed that the position of *Sema3c*-expressing NCCs corresponded to that of NCCs expressing PLXNA2 (compare Figure 5B with Figure 5C). We next generated conditional *Sema3c*-null mice (*Sema3c*$^{fl/fl}$) and crossed them to *Wnt1-Cre* mice. ISH at E12.5 showed that *Sema3c* expression was abolished in the *Wnt1-Cre Sema3c*$^{fl/fl}$ septal bridge (Figure 5C), consistent with cardiac NCCs providing a source of SEMA3C. In contrast, *Wnt1-Cre Sema3c*$^{fl/fl}$ mutants preserved *Sema3c* expression in the myocardial cuff, which is of SHF origin (Figure 5C). Quantitation of *Sema3c* mRNA levels confirmed a significant reduction in *Wnt1-Cre Sema3c*$^{fl/fl}$ mutants compared with controls (Figure 5D; *Sema3c*, normalized to *Gapdh* expression: 100% ± 10.1% *Sema3c*$^{fl/fl}$ versus 68% ± 13.8% *Wnt1-Cre Sema3c*$^{fl/fl}$; $P < 0.01$). Together, these findings raised the possibility that SEMA3C, rather than attracting cardiac NCCs into the OFT, is secreted by cardiac NCCs to promote OFT septation.

Cardiac NCC–derived SEMA3C is essential for proximal OFT septation. To investigate whether cardiac NCC–derived SEMA3C is essential for OFT septation, we immunolabeled serial sections of *Wnt1-Cre Sema3c*$^{fl/fl}$ OFTs for PECAM and SMA; this analysis demonstrated that septation was defective in the proximal OFT of all mutants examined (Figure 6A). As observed for *Nrp1*-null mutants, *Wnt1-Cre Sema3c*$^{fl/fl}$ mutants showed abnormal associations between the OFT endothelium and myocardium, causing cushion disorganization (Figure 6A). Furthermore, SMA-positive cells failed to invade the septal bridge; instead, they appeared to stall within the endocardial cushions in the lateral OFT (Figure 6, A and B), as observed for *Nrp1*-null mutants. However, OFT septation did occur more distally in 18 of 20 *Wnt1-Cre Sema3c*$^{fl/fl}$ mutants analyzed.

Previous observations that SEMA3C binds both NRP1 and NRP2 (27) and that OFT septation occurs normally in *Nrp2*$^{-/-}$ mutants or *Nrp1*$^{Sema/Sema}$ mutants with a knockin mutation that impairs semaphorin binding to NRP1 (13), but is defective in *Nrp1*$^{Sema/Sema}$ *Nrp2*$^{-/-}$ compound mutants, raised the possibility that SEMA3C signals with partial redundancy through NRP1 and NRP2 in the OFT. However, prior work examined neither which specific aspects of OFT septation were defective in double mutants nor whether their defects were similar to those of *Sema3c* mutants. Immunolabeling of serial sections showed similar anatomical OFT defects in *Nrp1*$^{Sema/Sema}$ *Nrp2*$^{-/-}$ compared with *Wnt1-Cre Sema3c*$^{fl/fl}$ mutants, including a failure of proximal OFT septation, which was accompanied by the formation of disorganized endocardial cushions and impaired myocardialization (Figure 6, A and B). This observation is consistent with cardiac NCC–derived SEMA3C signaling through NRP1 to enable OFT septation, whereby NRP2 is able to compensate for the failure of *Nrp1*^{Sema} to bind SEMA3C.

SEMA3C signaling through NRP1 is not required to regulate proliferation or apoptosis during OFT septation. Prior studies have shown that deletion of the BMP receptor ALK2 (ACVR1) or the TGF-β receptor ALK5 (TGFBR1) increases NCC apoptosis in the OFT and causes OFT defects (28, 29). Likewise, loss of the retinoid X receptor α increases apoptosis in the endocardial cushions and compromises OFT remodeling (30). Conversely, loss of FOX1P reduces apoptosis in the endocardial cushions and also causes OFT septation defects (31). We therefore immunolabeled OFT sections of mutants lacking NRP1 or NCC-derived SEMA3C for the apoptosis marker cleaved caspase 3 (aCAS3) (32, 33) at E11.5, prior to the stage when the OFT defect manifests itself in NRP1 mutants. Consistent with previous studies (34, 35), we observed little apoptosis in the OFT at E11.5 (Supplemental Figure 1A and Supplemental Figure 2A; supplemental material available online with this article; doi:10.1172/JCI79668DS1), with no significant difference in apoptosis between *Nrp1*-null and control OFTs (Supplemental Figure 1B; aCAS3-positive cells per OFT section: 2.75% ± 1.06% *Nrp1*$^{+/+}$ versus 2.83% ± 0.26% *Nrp1*$^{-/-}$; mice were on a CD1 background) or between *Wnt1-Cre Sema3c*$^{fl/fl}$ mutant and control OFTs (Supplemental Figure 2B; aCAS3-positive cells per OFT section: 9.95% ± 0.72% *Sema3c*$^{fl/fl}$ versus 9.2% ± 0.52% *Wnt1-Cre Sema3c*$^{fl/fl}$; mice were on a C57/BL6 background).

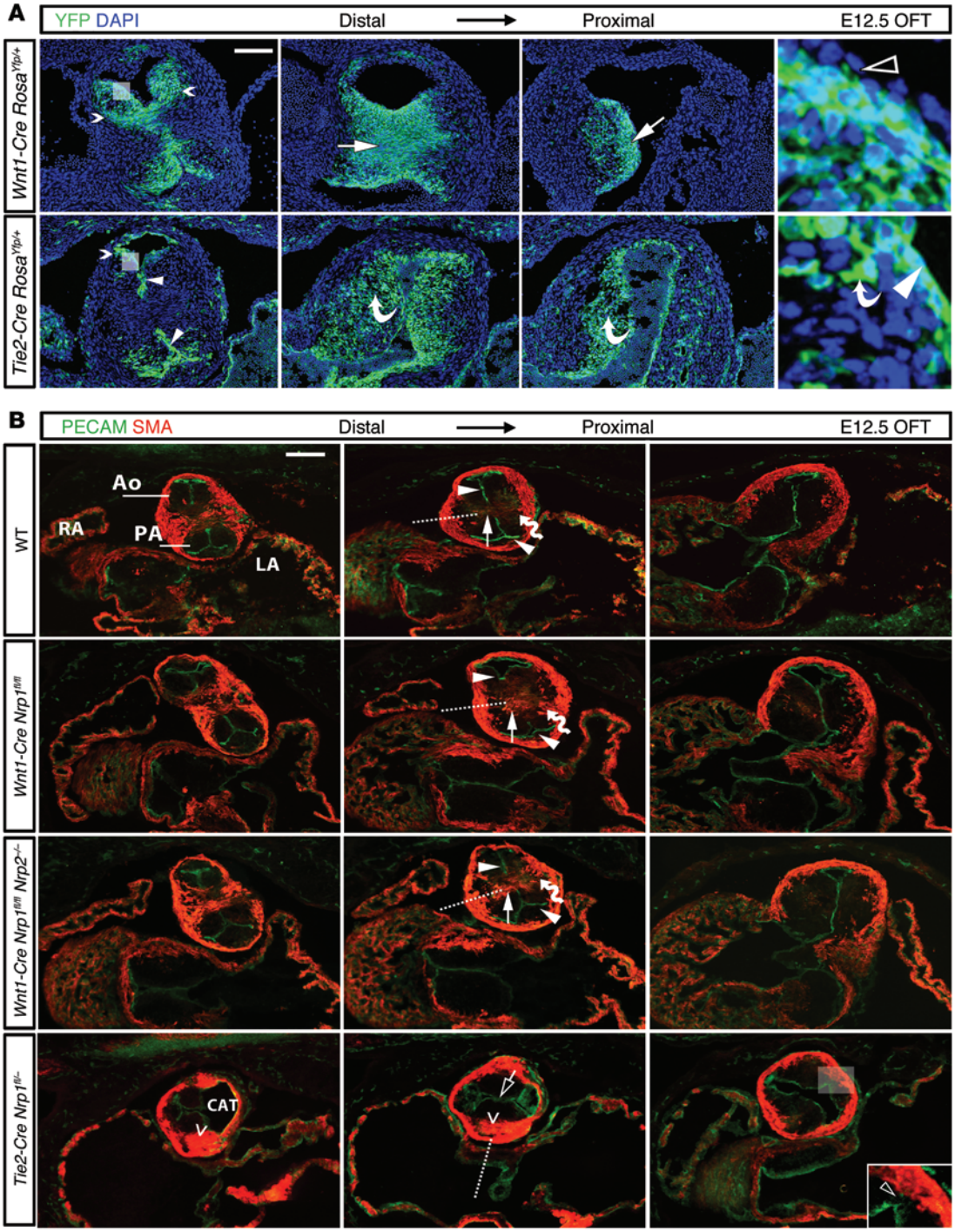

Figure 3. Endothelial-, not NCC-derived NRP1 enables OFT septation. (**A**) Serial sections of *Wnt1-Cre Rosa*^{Yfp} and *Tie2-Cre Rosa*^{Yfp} E12.5 OFTs at corresponding distal, medial, and proximal levels, labeled for YFP and DAPI. Angles and solid arrows highlight NCC contribution to the valves and septal bridge, respectively; solid arrowheads indicate endothelium of the aorta and pulmonary artery; and curved arrows indicate cells undergoing endoMT. Note the overlap of NCC position and endoMT in the proximal OFT. Shaded areas are shown in higher magnification on the right, with open and solid arrowheads indicating absence and presence of endothelial targeting, respectively. (**B**) Serial sections of *Wnt1-Cre Nrp1*$^{fl/fl}$ (n = 4), *Wnt1-Cre Nrp1*$^{fl/fl}$ *Nrp2*$^{-/-}$ (n = 3), *Tie2-Cre Nrp1*$^{fl/fl}$ (n = 6), and control (n = 7) E12.5 OFTs of the indicated genotypes, immunolabeled for PECAM and SMA. Solid arrowheads indicate endothelium of the aorta and pulmonary artery; solid arrows indicate septal bridge myocardialization; and open arrows indicate absence of septal bridge formation. Wavy arrows highlight migrating SMA-positive cells, while the angle highlights stalled SMA-positive cells. Dotted lines indicate the axis of OFT septation, and the open arrowhead indicates an atypical association between endothelium and myocardium. Scale bars: 100 μm (**A**); 200 μm (**B**).

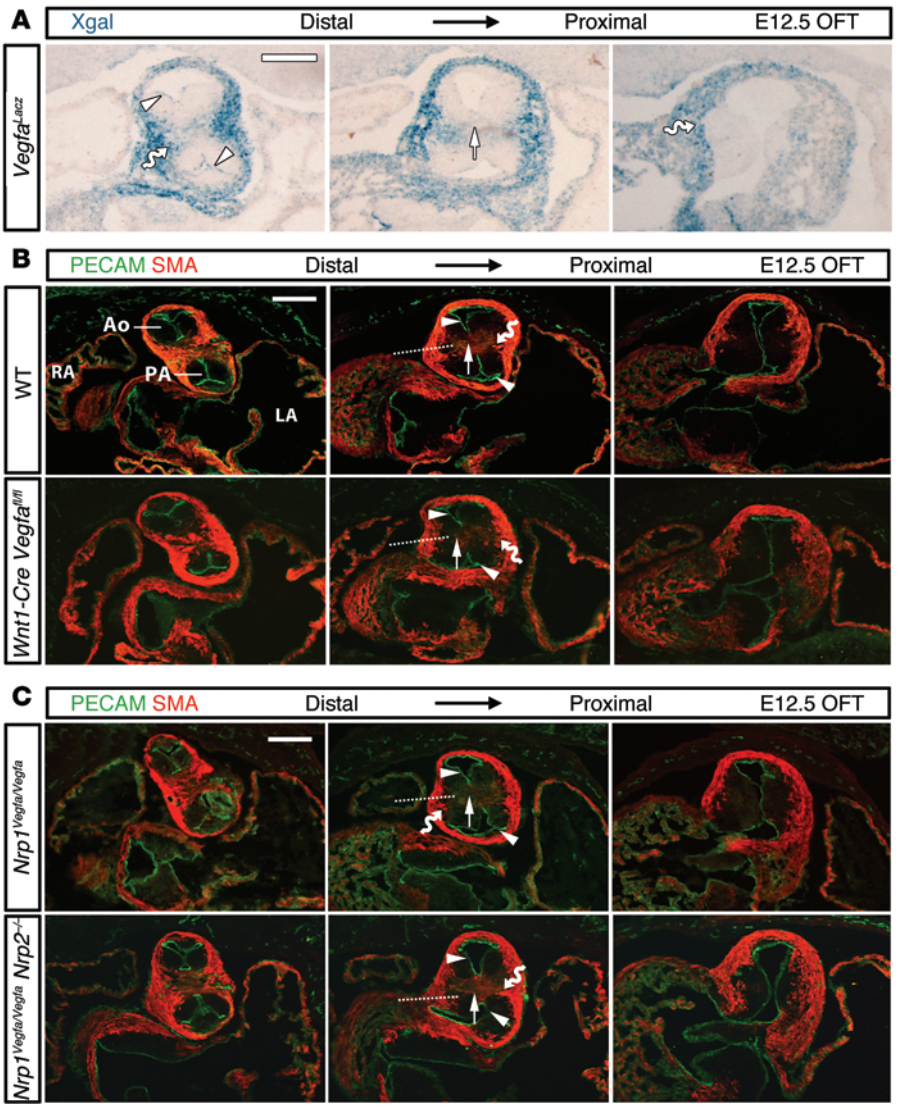

Figure 4. VEGF-A signaling through NRP1 is dispensable for OFT septation. (**A**) Serial sections through E12.5 *Vegfa*^{Lacz} OFTs stained with X-gal. Arrowheads indicate weak *Vegfa* expression by OFT endothelium; wavy arrows indicate *Vegfa* expression by the OFT myocardium; and the arrow indicates lack of *Vegfa* expression in the septal bridge area. (**B** and **C**) Serial sections of E12.5 OFTs of the indicated genotypes, immunolabeled for PECAM and SMA. Arrowheads indicate endothelium of the aorta and pulmonary artery, while arrows highlight septal bridge myocardialization. Wavy arrows highlight migrating SMA-positive cells and dotted lines the axis of septal bridge formation. Scale bars: 200 μm (**A**–**C**).

Defects in proliferation may also cause OFT defects. Thus, deletion of the BMP type 1 receptor in NCCs reduces proliferation in the endocardial cushions and correlates with defective OFT remodeling (36). We therefore used the proliferation marker phosphohistone H3 (pHH3) (37, 38) to label E11.5 OFT sections of *Nrp1*-null mutants and their littermates (Supplemental Figure 1C), but found no significant difference (Supplemental Figure 1D; pHH3-positive cells per OFT section: 13.5% ± 3.54% *Nrp1*$^{+/+}$ versus 12.88% ± 1.24% *Nrp1*$^{-/-}$). There was also no significant difference in the number of proliferating cells between *Wnt1-Cre Sema3c*$^{fl/fl}$ mutant and control OFTs (Supplemental Figure 2, C and D; pHH3-positive cells per OFT section: 6.36% ± 0.7% *Sema3c*$^{fl/fl}$ versus 6.58% ± 1.25% *Wnt1-Cre Sema3c*$^{fl/fl}$).

NRP1 is not required for cardiac NCC migration into the OFT. The surprising lack of OFT defects in *Wnt1-Cre Nrp1*$^{fl/fl}$ mutants (Figure 3B) prompted us to investigate in more detail whether NRP1 is required for cardiac NCC migration into the mouse OFT, as reported for chick (14). X-gal staining of E10.5 OFTs containing the NCC reporter *Wnt1-Cre Rosa*^{Lacz} (39) showed that cardiac NCCs migrated through the pharyngeal arch arteries and into the OFT in 2 prong-shaped streams in both *Nrp1*-null mutant and control OFTs (Figure 7A). Furthermore, YFP immunostaining of serial sections through E10.5 WT OFTs carrying the *Wnt1-Cre Rosa*^{Yfp} reporter showed that cardiac NCCs had populated the OFT at this stage, with a similar pattern in stage-matched *Nrp1*-null mutants (Figure 7B). Quantitation of YFP-positive cells confirmed that a similar number of cardiac NCCs had populated the OFT in both genotypes (Figure 7C; YFP^{+} cells relative to control: *Nrp1*$^{+/+}$ 100% ± 12.2% versus *Nrp1*$^{-/-}$ 104.3% ± 25.3%). These findings imply that the OFT defect of *Nrp1*$^{-/-}$ mutants is not caused by impaired cardiac NCC migration into the OFT.

SEMA3C signaling through NRP1 promotes NCC-dependent septal bridge formation. Because immunolabeling had shown that PLXNA2 visualizes SEMA3C-expressing cardiac NCCs (Figure 5B), we used this marker to examine cardiac NCC behavior in NRP1 and SEMA3C mutants. PLXNA2-labeled sections through E12.5 WT OFTs confirmed that cardiac NCCs were localized in the OFT center at this stage (Figure 8A). Moreover, the entry of cardiac NCCs into the septal bridge appeared to precede the invasion of SMA-positive cells from the myocardial cuff into this area, whereby the invading SMA-positive cells seemed to orient themselves toward the cardiac NCCs (Figure 8A). These findings suggest a role for cardiac NCCs in attracting SMA-positive cells into the bridge area to initiate the process of myocardialization.

PLXNA2 immunostaining of full and endothelial-specific *Nrp1* mutants showed that cardiac NCCs had reached the OFT at E12.5 (Figure 8A). This observation agreed with the *Wnt1-Cre* lineage trace at E10.5, which had demonstrated that NRP1 expression by cardiac NCCs was not required to attract these cells into the OFT (Figure 7). Interestingly, however, PLXNA2-positive NCCs were localized in 2 lateral columns both in full and endothelial *Nrp1*-null OFTs at E12.5, rather than fusing in a central position as seen in WT at this stage (Figure 8A). The bilateral location of cardiac NCCs in mutants corresponded to the position of the 2

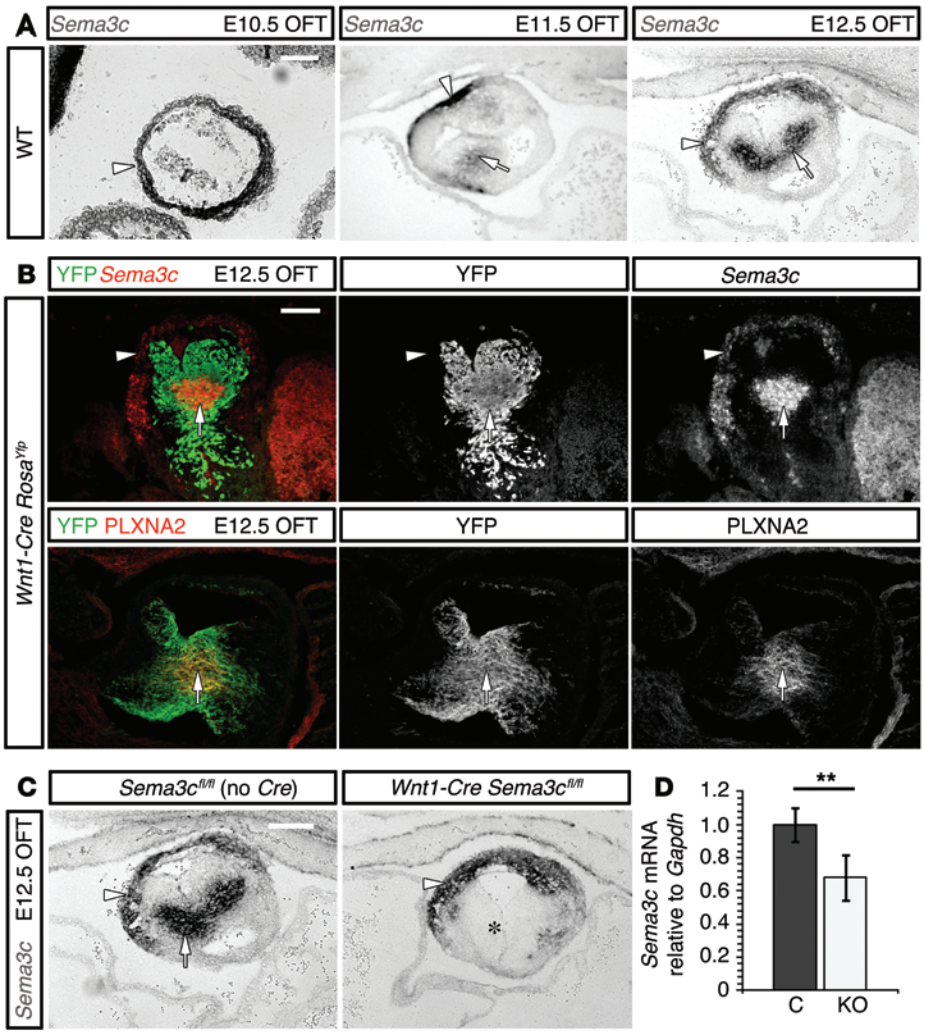

Figure 5. *Sema3C* expression by cardiac NCCs and myocardial cuff cells in the OFT. (**A**) *Sema3c* ISH on E10.5, E11.5, and E12.5 OFT sections. (**B**) Immunolabeling of sections through *Wnt1-Cre Rosa*^{Yfp} OFTs for YFP after *Sema3c* ISH (pseudocolored) or for YFP and PLXNA2; note partial colocalization of YFP with *Sema3C* and PLXNA2 staining in the septal bridge. (**C**) *Sema3c* expression in E12.5 OFTs from *Sema3c*$^{fl/fl}$ mice with or without the *Wnt1-Cre* transgene. Arrowheads and arrows indicate *Sema3c* expression in myocardial cuff cells and the septal bridge area, respectively. The asterisk indicates absent *Sema3c* in the septal bridge area. (**D**) Quantitation of *Sema3c* mRNA levels in E11.5 *Wnt1-Cre Sema3c*$^{fl/fl}$ and *Sema3c*$^{fl/fl}$ (n = 4 each) OFTs relative to *Gapdh*. Mean ± SD. $^{**}P \leq 0.01$, 2-tailed, unpaired Student's t test. Scale bars: 100 μm (**A**–**C**).

NCC prongs seen at E10.5 (Figure 7A), indicating a failure of NCC translocation to the central area. In addition, full and endothelial-specific *Nrp1* mutants showed defective SMA-positive cell migration, whereby these cells were no longer oriented toward the central area of the OFT; instead, they seemed to be attracted by the mispositioned NCCs (Figure 8A).

The findings above are consistent with the idea that NRP1 is dispensable for cardiac NCC attraction into the OFT, but instead NRP1 is required to initiate NCC relocalization from a lateral area into a central OFT position and the ensuing attraction of SMA-positive cells into this area for septal bridge formation. In agreement with this model and demonstrating that the NRP1 ligand directing cardiac NCC translocation is SEMA3C rather than VEGF-A, NCC migration into the central OFT was normal in *Nrp1*$^{Vegfa/Vegfa}$ *Nrp2*$^{-/-}$ mice lacking VEGF-A signaling through NRPs, but absent in *Nrp1*$^{Sema/Sema}$ *Nrp2*$^{-/-}$ mice lacking semaphorin signaling through NRPs (Figure 8A, bottom row). Moreover, mice lacking NCC-derived SEMA3C also lacked central NCC localization, with NCCs located in 2 lateral columns and abnormal SMA-positive cell migration toward the stalled NCCs (Figure 8A).

To investigate how ablation of SEMA3C/NRP1 signaling in the OFT endothelium affects the behavior of the total cardiac NCC population, including NCCs that do not express SEMA3C or PLXNA2, we introduced the *Wnt1-Cre Rosa*^{Yfp} reporter into *Nrp1*-null or *Sema3c*$^{fl/fl}$ mice and stained E12.5 sections for YFP and the SMC and myocyte marker SM22α. As observed with PLXNA2 and X-gal staining, YFP staining suggested that a similar number of cardiac NCCs had migrated into the OFT of *Nrp1*$^{-/-}$ mice and WT littermates (Figure 8B). Despite having reached the OFT, fewer YFP-positive cells had relocalized into the central area of the *Nrp1*-null mutant OFT at E12.5 (Figure 8B), consistent with the results obtained by PLXNA2 staining at E12.5 (Figure 8A). Impaired relocalization of YFP-positive cells was also observed in the proximal OFT of *Wnt1-Cre Rosa*^{Yfp} *Sema3c*$^{fl/fl}$ mutants (Figure 8B). These observations suggest that the SEMA3C-expressing cardiac NCC subset is key for septal bridge formation and the attraction of SMA-positive cells for myocardialization into the proximal OFT. Whereas NCC-derived SEMA3C was essential for cardiac NCC relocalization in the proximal OFT, cardiac NCCs had successfully migrated into the central area in the distal OFT of *Wnt1-Cre Rosa*^{Yfp} *Sema3c*$^{fl/fl}$ mutants (Figure 8B). This observation agrees with the incomplete penetrance of septation in the distal OFT of *Wnt1-Cre Sema3c*$^{fl/fl}$ and *Nrp1*$^{Sema/Sema}$ *Nrp2*$^{-/-}$ mutants and suggests that factors other than NCC-derived SEMA3C can contribute to distal OFT septation (see Discussion).

Together, these findings demonstrate that semaphorin, not VEGF-A signaling through NRP1, is a major driving force underlying NCC-mediated OFT septation. Moreover, they imply that NCC-derived SEMA3C signals to endothelial NRP1 to indirectly promote cardiac NCC relocalization toward the center of the proximal OFT, which is followed by the invasion of SMA-positive cells and therefore the formation of a myocardialized septal bridge.

NCC colonization of the OFT correlates with the onset of endoMT. The results above show that mice with impaired SEMA3C/NRP1

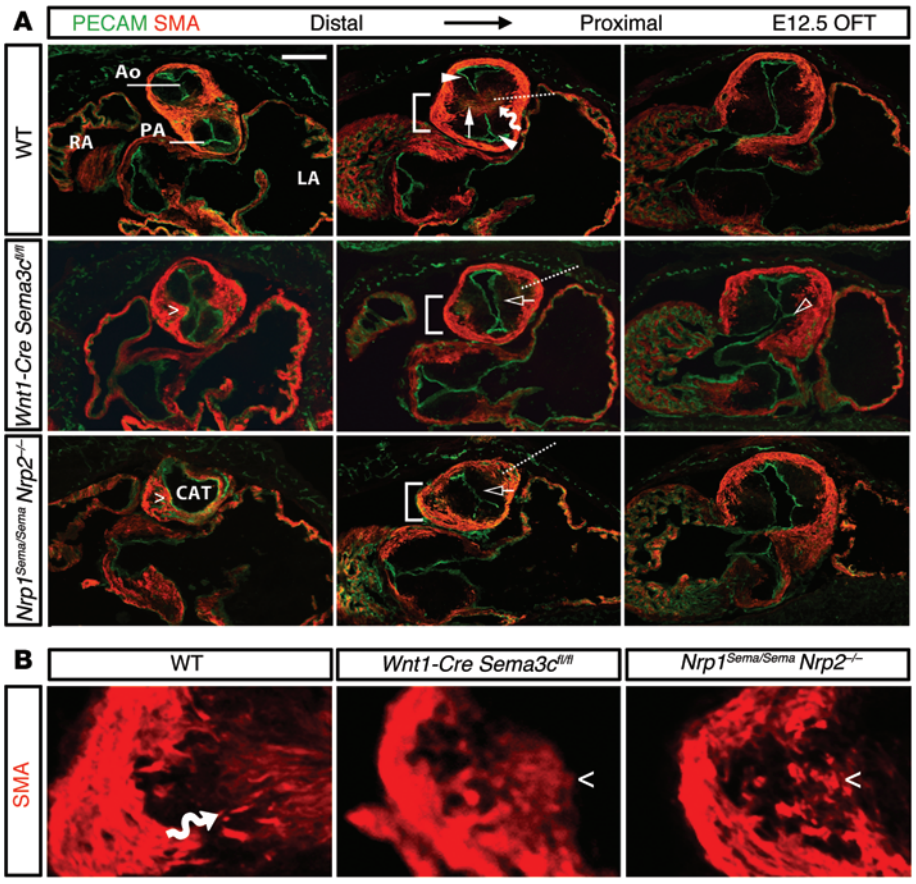

Figure 6. Cardiac NCC–derived SEMA3C signals through NRP1 to promote OFT septation. (**A** and **B**) Serial sections through *Wnt1-Cre Sema3c*$^{fl/fl}$ and *Sema3c*$^{fl/fl}$ control (n = 20 each). E12.5 OFTs were immunolabeled for PECAM and SMA and imaged at corresponding proximal, medial, and distal levels. The area indicated with a square bracket in **A** is shown in higher magnification as single SMA channel in **B**. Solid arrowheads indicate endothelium of the aorta and pulmonary artery; the solid arrow indicates septal bridge myocardialization; and open arrows indicate absence of septal bridge formation. Wavy arrows highlight the migrating SMA-positive cells, and the angles indicate stalled SMA-positive cells. The dotted lines indicate the axis of septal bridge formation, and the open arrowheads indicate an atypical association between the endocardium and the myocardium. Scale bar: 200 μm (**A**).

signaling lacking NCC-derived SEMA3C display disorganized endocardial cushions and lack proximal OFT septation, 2 processes known to rely on endoMT (17–19). We therefore investigated whether cardiac NCC immigration and the onset of endoMT correlate during OFT development. Using *Wnt1-Cre* lineage tracing, we observed that YFP-positive NCCs at E10.5 had colonized the OFT and were present even within the most proximal segment of the OFT (Figure 9A). We then used the *Tie2-Cre Rosa*^{Yfp} reporter to identify endoMT-derived cells by their YFP expression in the absence of PECAM (Figure 3A). This analysis revealed that *Tie2-Cre* targeted the OFT endothelium at E10.5 (Figure 9B), but only few YFP-positive, PECAM-negative single cells were present in the endocardial cushions (Figure 9B). In contrast, E12.5 OFTs contained many single cells that were YFP positive, but lacked PECAM (Figure 9C), demonstrating that they had arisen through endoMT. EndoMT therefore begins in the OFT at E10.5, when cardiac NCCs have already populated the entire length of the OFT. Moreover, the onset of endoMT correlates with a time when cardiac NCC began to express *Sema3c* in the OFT (see above, Figure 5A).

SEMA3C signals through NRP1 to induce endoMT of OFT endothelium in vitro. To investigate whether SEMA3C induces endoMT in the OFT in an NRP1-dependent manner, we used an established in vitro assay in which endoMT from explanted OFT tissue is measured as F-actin–positive cellular outgrowth (17, 40, 41). Accordingly, we found that explants of *Tie2-Cre Rosa*^{Yfp} OFTs at E10.5, when endoMT just begins (Figure 9B), gave rise to F-actin–positive outgrowth cells, most of which were YFP positive, but PECAM negative, consistent with endoMT (Figure 9, D and E). OFT explants from *Wnt1-Cre Sema3c*$^{fl/fl}$ mice lacking SEMA3C expression in cardiac NCCs showed significantly reduced F-actin–positive outgrowth compared with control explants (Figure 9F; outgrowth cells relative to control: 100% ± 4.5% *Sema3c*$^{fl/+}$ versus 72% ± 7.6% *Wnt1-Cre Sema3c*$^{fl/fl}$; $P < 0.01$). We also observed significantly reduced F-actin–positive outgrowth in *Nrp1*-null explants compared with controls (Figure 9G; outgrowth cells relative to control: 100% ± 5.6% *Nrp1*$^{+/+}$ versus 62.7% ± 5.5% *Nrp1*$^{-/-}$; $P < 0.001$).

We next determined whether exogenous SEMA3C promoted endoMT in OFT explants. For this experiment, we cultured E10.5 WT OFTs for 72 hours in medium containing 1% serum and found that SEMA3C significantly promoted F-actin–positive cellular outgrowth (Figure 9H; percentage of outgrowth cells relative to control: 100% ± 3.9% WT versus 186% ± 25.6% WT + SEMA3C; $P < 0.01$). In contrast, OFT explants from *Nrp1*-null mutant littermates did not increase reduced F-actin–positive outgrowth in response to SEMA3C (Figure 9I; percentage of outgrowth cells relative to control: 100% ± 5.8% *Nrp1*$^{+/+}$ + SEMA3C versus 71.7% ± 15.8% *Nrp1*$^{-/-}$ + SEMA3C; $P < 0.05$). Furthermore, a direct comparison of *Nrp1*$^{-/-}$ explants with and without SEMA3C treatment showed that F-actin–positive outgrowth in *Nrp1* mutants was not affected by SEMA3C treatment (percentage of outgrowth cells relative to control: 62.7% ± 5.5% *Nrp1*$^{-/-}$ versus 71.7% ± 15.8% *Nrp1*$^{-/-}$ + SEMA3C; $P > 0.05$). This experiment demonstrated that SEMA3C promoted F-actin–positive outgrowth in WT, but not *Nrp1*-null mutant explants, and suggested that cardiac NCC–derived SEMA3C enhances endoMT in the OFT via NRP1.

Reduced endoMT in the OFT of mice lacking SEMA3C or NRP1 in vivo. To show that endoMT was reduced in the OFT of mice lacking NRP1 in vivo, we investigated the expression of the transcription factor *Slug*, a well-established effector of endoMT (42, 43). We first performed reverse-transcription PCR (RT-PCR) analysis

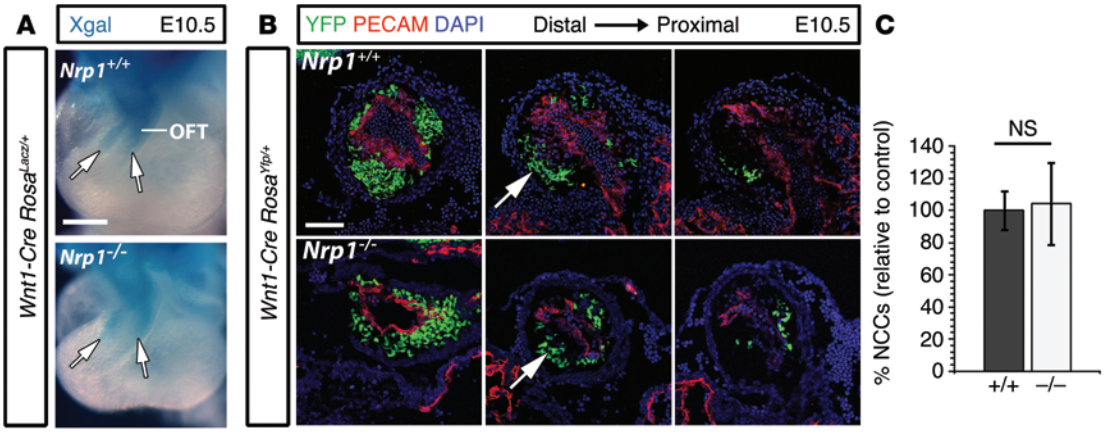

Figure 7. NRP1 is dispensable for NCC migration into the OFT. (**A**) Whole-mount X-gal staining of *Wnt1-Cre Rosa*^{Lacz} E10.5 OFTs on a WT or *Nrp1*-null background (n = 3 each). (**B**) Serial sections through OFTs of E10.5 *Wnt1-Cre Rosa*^{Yfp} mice on a WT and *Nrp1*-null background immunolabeled for YFP and PECAM and counterstained with DAPI. Arrows indicate migrating NCCs. Scale bars: 200 μm (**A**); 100 μm (**B**). (**C**) Quantitation of YFP-positive cells in *Nrp1*-null mice relative to control E10.5 OFTs (n = 3 each) on a *Wnt1-Cre Rosa*^{Yfp} background. Mean ± SD, 2-tailed, unpaired Student's t test.

on *Nrp1*-null and control OFTs at E10.5, when endoMT is initiated (Figure 9B). This experiment suggested reduced *Slug* expression in *Nrp1*-null mice compared with control littermates (Figure 10A). Quantitative real-time RT-PCR (qRT-PCR) analysis of E10.5 OFT tissue confirmed that *Slug* was significantly reduced in mutants compared with controls (Figure 10B; *Slug* mRNA levels relative to control and normalized to *Gapdh* expression: 1% ± 0.09% *Nrp1*$^{+/-}$ versus 0.69% ± 0.15% *Nrp1*$^{-/-}$; $P < 0.05$). *Slug* was also significantly reduced in the OFT of E10.5 *Wnt1-Cre Sema3c*$^{fl/fl}$ mutants compared with control littermates (Figure 10C; *Slug* levels relative to control and normalized to *Gapdh* expression: 1% ± 0.2% *Sema3c*$^{fl/fl}$ versus 0.6% ± 0.27% *Wnt1-Cre Sema3c*$^{fl/fl}$; $P < 0.05$).

We also performed immunostaining of E11.25 serial OFT sections for PECAM and a previously validated antibody for SLUG (44). WT OFTs contained many SLUG-positive cells, particularly in areas close to the endothelium, but also surrounding the areas where the paired NCC columns reside at this stage (Figure 10D). Staining appeared to be mostly nuclear, in keeping with SLUG's role as a transcription factor and in agreement with prior reports (44–46). In contrast, *Nrp1*-null OFTs contained fewer SLUG-positive single cells immediately adjacent to the OFT endothelium (Figure 10D), consistent with the hypothesis that NRP1 promotes endoMT in the OFT. Immunolabeling of E11.25 OFTs also revealed fewer SLUG-positive single cells near OFT endothelium in *Wnt1-Cre Sema3c*$^{fl/fl}$ mutant compared with control OFTs (Supplemental Figure 3).

Intriguingly, SLUG labeling of *Nrp1*-null OFTs suggested that many SLUG-positive cells were retained within the OFT endothelium (Figure 10D). This observation raised the possibility that defective endoMT induction at E10.5 caused endothelial retention of cells that are normally destined for endoMT. Moreover, SLUG staining, rather than being nuclear, appeared predominantly cytoplasmic in the OFT endothelium of *Nrp1*-null mutants (Figure 10D). A similar staining pattern was previously observed in cells with impaired SLUG phosphorylation (47), raising the possibility that cytoplasmic SLUG staining in *Nrp1*-null OFTs reflects dysregulated signaling.

Reduced *Slug* expression at E10.5 and the abnormal distribution of SLUG-positive cells at E11.25 predicted fewer mesenchymal cells of endothelial origin in the absence of endothelial NRP1 activation by SEMA3C. To test this idea and validate the predictions of the OFT explant assays (Figure 9), we visualized cells that had arisen by endoMT in the E12.5 OFT of endothelial *Nrp1*-null mutants through *Tie2-Cre Rosa*^{Yfp} lineage tracing. Immunostaining of serial sections showed that the area occupied by YFP-positive, PECAM-negative cells was significantly smaller in the endocardial cushions in mutants compared with controls (Figure 10, E and F; YFP$^+$ PECAM$^-$ area: 100% ± 12.6% *Nrp1*$^{fl/fl}$ versus 65.1% ± 18.2% *Tie2-Cre Nrp1*$^{fl/-}$; $P < 0.05$). Taken together, these observations show that endothelial NRP1 is required for normal levels of endoMT in the developing mouse OFT in vivo.

Discussion

Even though the importance of NRP1 for OFT remodeling and therefore cardiovascular function has been recognized for more than a decade (11), its mechanism of action was not previously understood. A widely accepted hypothesis postulated that NRP1 contributes to OFT remodeling in a dual fashion: first, by enabling the SEMA3C-mediated attraction of NRP1-expressing cardiac NCCs into the OFT, and second, by acting as a VEGF-A receptor in NRP1-expressing OFT endothelium to induce an unidentified endothelial function. By taking advantage of a hitherto unavailable repertoire of tissue-specific and ligand-selective *Nrp1* mouse mutants and analyzing them through in vivo and in vitro approaches, we have now overhauled the prior working model and defined roles for NRP1 in OFT septation. First, we found that neither NRP1 nor NRP2 is required to guide cardiac NCCs into the mouse OFT. Second, we demonstrated that endothelial NRP1 is not required as a receptor for VEGF-A during OFT remodeling, but that this process instead relies on SEMA3C signaling through NRP1 in OFT ECs. Third, we identified a hitherto unrecognized role for NCC-derived SEMA3C and endothelial NRP1 in promoting endoMT in the OFT and therefore the generation of mesenchymal cells for the endocardial cushions. Finally, we found that SEMA3C signal-

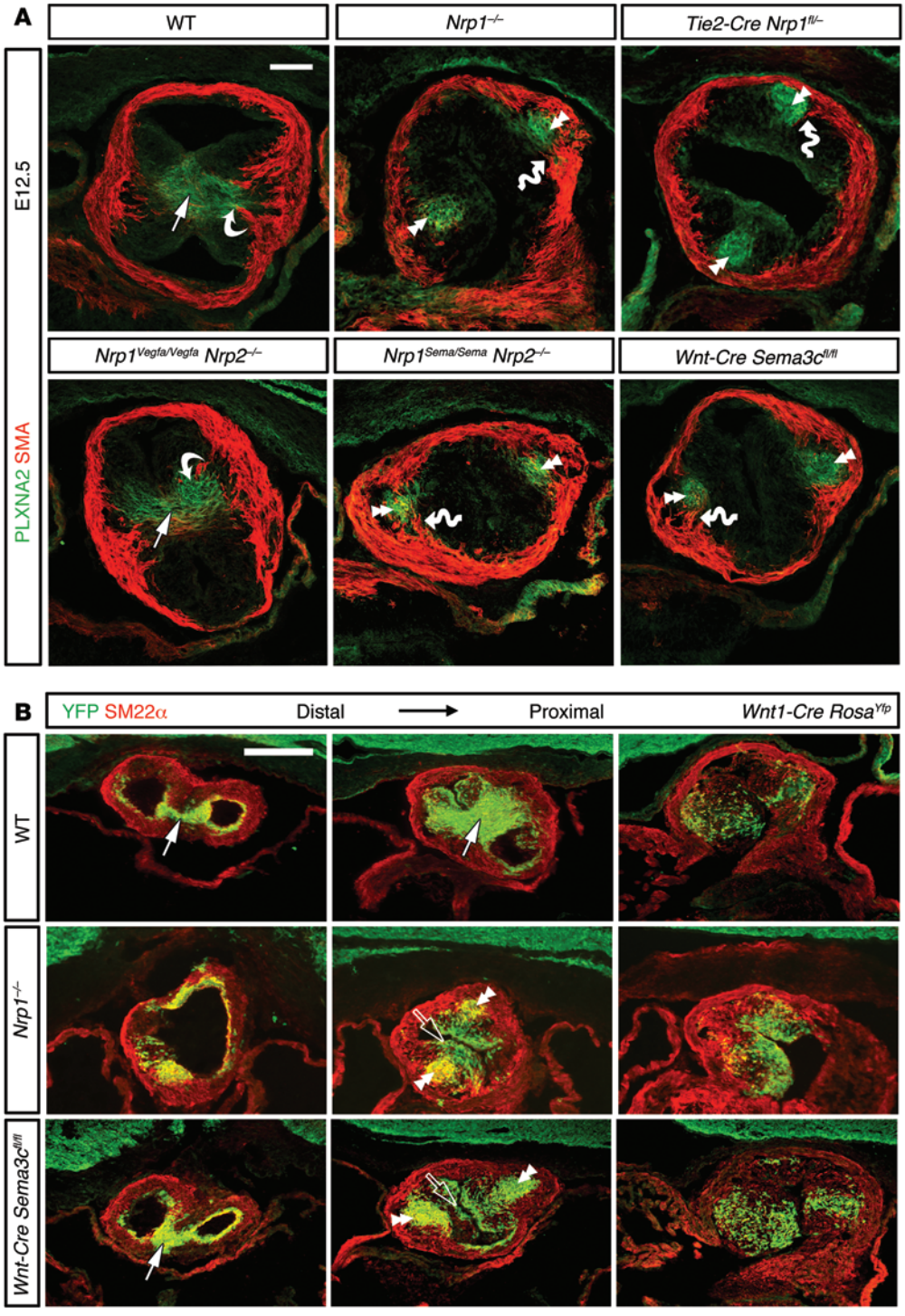

Figure 8. SEMA3C signals through NRP1 to promote convergence of cardiac NCCs and septal bridge myocardialization. E12.5 OFT sections of the indicated genotypes were immunolabeled for PLXNA2 and SMA (**A**) or YFP and the early SMC and myocyte marker SM22α (**B**). Arrows indicate NCCs in the septal bridge in WTs (n = 6) and mice lacking VEGF-A or SEMA3C signaling through NRPs (n = 3 each). Curved arrows highlight SMA-positive cells migrating toward centrally located NCCs, and wavy arrows indicate SMA-positive cells migrating toward abnormal lateral NCCs in **A**. Double arrowheads denote the abnormal lateral position of NCCs in the other genotypes, while the open arrow in **B** indicates a smaller population of neural crest–derived cells that do not express PLXNA2, as shown in **A**, which still migrate toward the central OFT, but are not sufficient to induce proximal OFT septation. Mean ± SD, 2-tailed, unpaired Student's t test. Scale bars: 100 μm.

ing through NRP1 is required for the fusion of the bilateral cardiac NCC columns in the central OFT to enable the formation and myocardialization of the septal bridge that separates the emerging aortic and pulmonary trunks.

Genetic knockout studies have previously implicated SEMA3C as a critical factor for OFT septation (8). Because SEMA3C binds both NRPs with similar affinity (27, 48), the occurrence of CAT in *Nrp1*$^{Sema/Sema}$ *Nrp2*$^{-/-}$ mice was thought to indicate that SEMA3C acts on cells that express both NRPs. In particular, it was suggested that these SEMA3C-dependent cells are cardiac NCCs (13, 14). According to this prior model, mice lacking NRP1 and NRP2 in NCCs should show impaired cardiac NCC migration into the OFT and therefore defective OFT septation, similar to *Sema3c*-null mice. However, *Wnt1-Cre Nrp1*$^{fl/fl}$ *Nrp2*$^{-/-}$ mutants lacking semaphorin signaling through both NRPs had normal cardiac NCC migration and OFT septation, excluding the possibility that semaphorin signaling through NRPs is required for cardiac NCC immigration into the developing OFT of mice. The finding that *Wnt1-Cre Nrp1*$^{fl/fl}$ *Nrp2*$^{-/-}$ mutants had normal cardiac NCC migration into the OFT disagrees with prior studies in chick, in which siRNA-mediated NRP1 targeting impaired this process (14). This discrepancy might be due to species differences in cardiac NCC behavior. In support of this idea, the misregulation of SDF1 or its receptor CXCR4 also perturbs cardiac NCC migration in chick (49), whereas the corresponding mouse mutants display only mild anomalies (50, 51). Alternatively, the siRNA-mediated knockdown technology used for the chick studies may have sensitized NCCs to developmental defects.

In contrast to *Wnt1-Cre Nrp1*$^{fl/fl}$ *Nrp2*$^{-/-}$ mice, *Tie2-Cre Nrp1*$^{fl/-}$ mutants fully recapitulated the OFT defects of full *Nrp1*-null

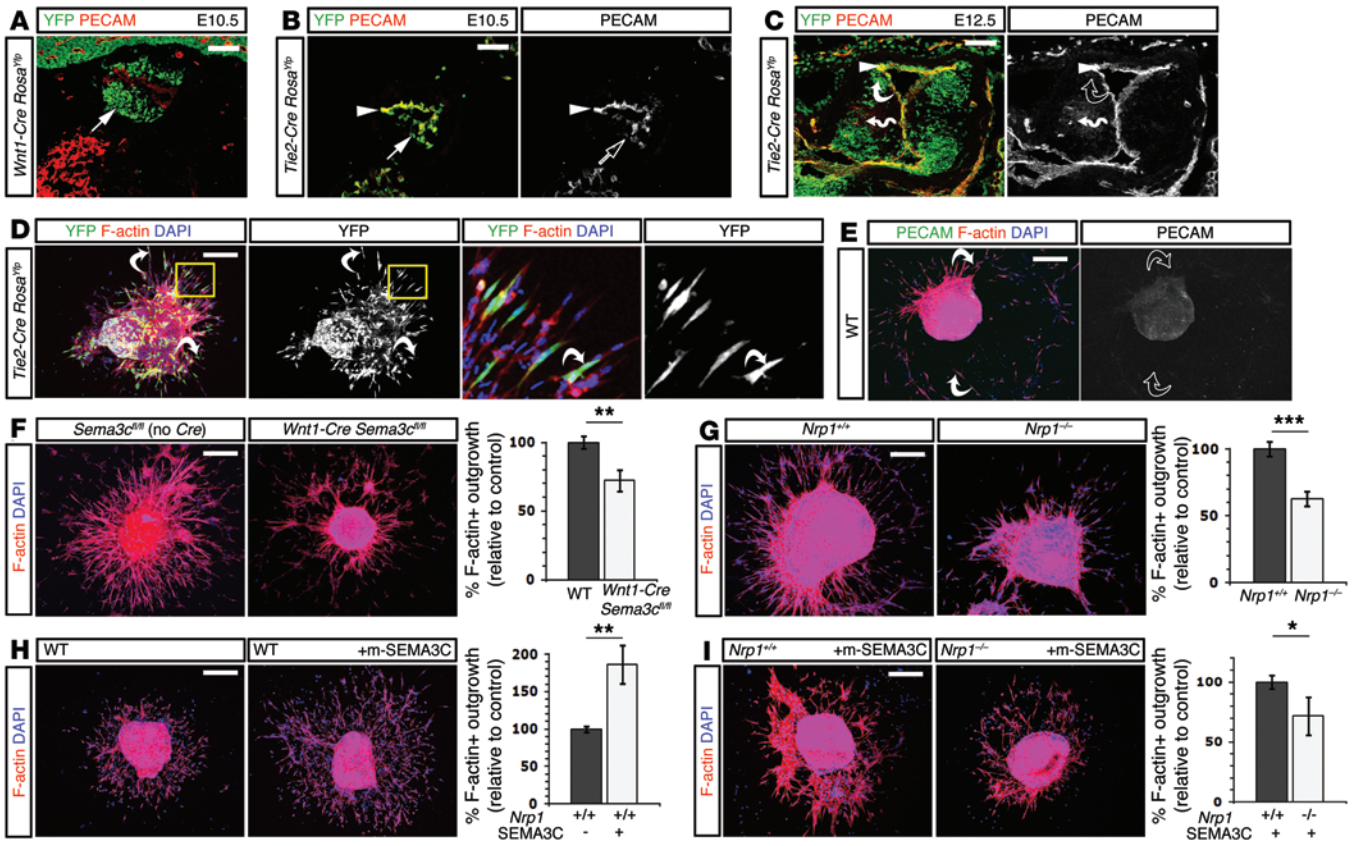

Figure 9. SEMA3C signals via NRP1 to induce endoMT of OFT endothelium. OFT sections from E10.5 *Wnt1-Cre Rosa*^{Yfp} (**A**) and *Tie2-Cre Rosa*^{Yfp} mice at E10.5 and E12.5 (**B** and **C**) were immunolabeled for YFP and PECAM. Arrows indicate YFP-positive cells within the endocardial cushions; arrowheads indicate YFP-positive OFT endothelium. Curved arrows highlight YFP-positive cells that have undergone endoMT; the open curved arrow shows a lack of PECAM expression in these cells. The wavy arrow labels PECAM-positive capillaries. (**D** and **E**) E10.5 OFT explants of the indicated genotypes were labeled for F-actin and YFP (**D**) or PECAM (**E**) and counterstained with DAPI after 72 hours of culture. Curved arrows indicate YFP-positive outgrowth cells, demonstrating their origin by endoMT, while open curved arrows show that outgrowth cells lack PECAM after endoMT. (**F** and **G**) E10.5 *Wnt1-Cre Sema3c*$^{fl/fl}$ (n = 6) (**F**) and *Nrp1*-null (n = 5) (**G**) OFTs with their WT littermates (n = 14 and n = 4, respectively) were labeled for F-actin and DAPI after 72 hours of culture and the number of F-actin–positive emigrated cells quantitated. (**H** and **I**) E10.5 WT and *Nrp1*$^{-/-}$ OFTs (n = 3 each) were cultured for 72 hours in 1% FBS with or without 400 ng/ml SEMA3C and labeled for F-actin and DAPI. The number of F-actin–positive emigrated cells was quantitated. Mean ± SD. *$P \le 0.05$; **$P \le 0.01$; ***$P \le 0.001$, 2-tailed, unpaired Student's t test. Scale bars: 100 μm (**A** and **B**); 200 μm (**C**–**I**).

mice. This finding suggests that all major NRP1-dependent steps during OFT remodeling are orchestrated by endothelial NRP1, with no obvious NRP1-dependent roles for cardiac NCCs (and perhaps a minor role of NRP1 in SMA-positive cells during septal bridge myocardialization, which we have not investigated). Given the essential role of SEMA3C signaling through endothelial NRP1 in OFT septation, it is not immediately obvious why NRP2 is able to compensate for loss of semaphorin binding to NRP1, as observed in *Nrp1*$^{Sema/Sema}$ mice (13). One possibility is that NRP2 and NRP1 form a heterodimer, in which both NRPs function redundantly as SEMA3C receptors. In agreement, heterodimer formation has been demonstrated in Cos7 cells in vitro, where NRP1 and NRP2 preassemble in a ligand-independent fashion (27, 48, 52). In a heterodimeric complex, NRP2 may be sufficient to bind SEMA3C, even if the semaphorin-binding domain of NRP1 is disrupted; however, the remainder of the NRP1 receptor is likely indispensable for downstream signaling. In support of this model, *Nrp2*$^{-/-}$ mutants do not display defects in OFT remodeling (53) and NRP2 is not sufficient to substitute for the endothelial-specific or full *Nrp1*-null mutation, even though NRP2 can rescue the *Nrp1*^{Sema} mutation (11, 13).

NRP1 signaling in OFT endothelium appears to require a signal-transducing coreceptor because mice lacking the cytoplasmic tail of NRP1 are viable and should therefore lack OFT defects (54). This endothelial NRP1 coreceptor is likely PLXND1, because (a) both NRP1 and NRP2 form complexes with PLXND1, (b) PLXND1 enhances SEMA3C binding to NRP-expressing Cos7 cells, and (c) *Plxnd1*-null mice have OFT defects similar to those of NRP1 and SEMA3C knockouts (24). Moreover, the endothelial PLXND1 deletion, similar to the endothelial NRP1 deletion, recapitulates the OFT defects of constitutive *Plxnd1*-null mutants, demonstrating that the essential function of the NRP1/PLXND1 receptor complex occurs in OFT endothelium rather than in another cell type such as cardiac NCCs (55).

We also tested the prior hypothesis that NRP1 acts as a VEGF-A receptor in OFT endothelium (13). This hypothesis was an extrapolation of findings in ECs in vitro, in which NRP1 forms a complex with VEGFR2 to enhance VEGF-A signaling through VEGFR2 (56).

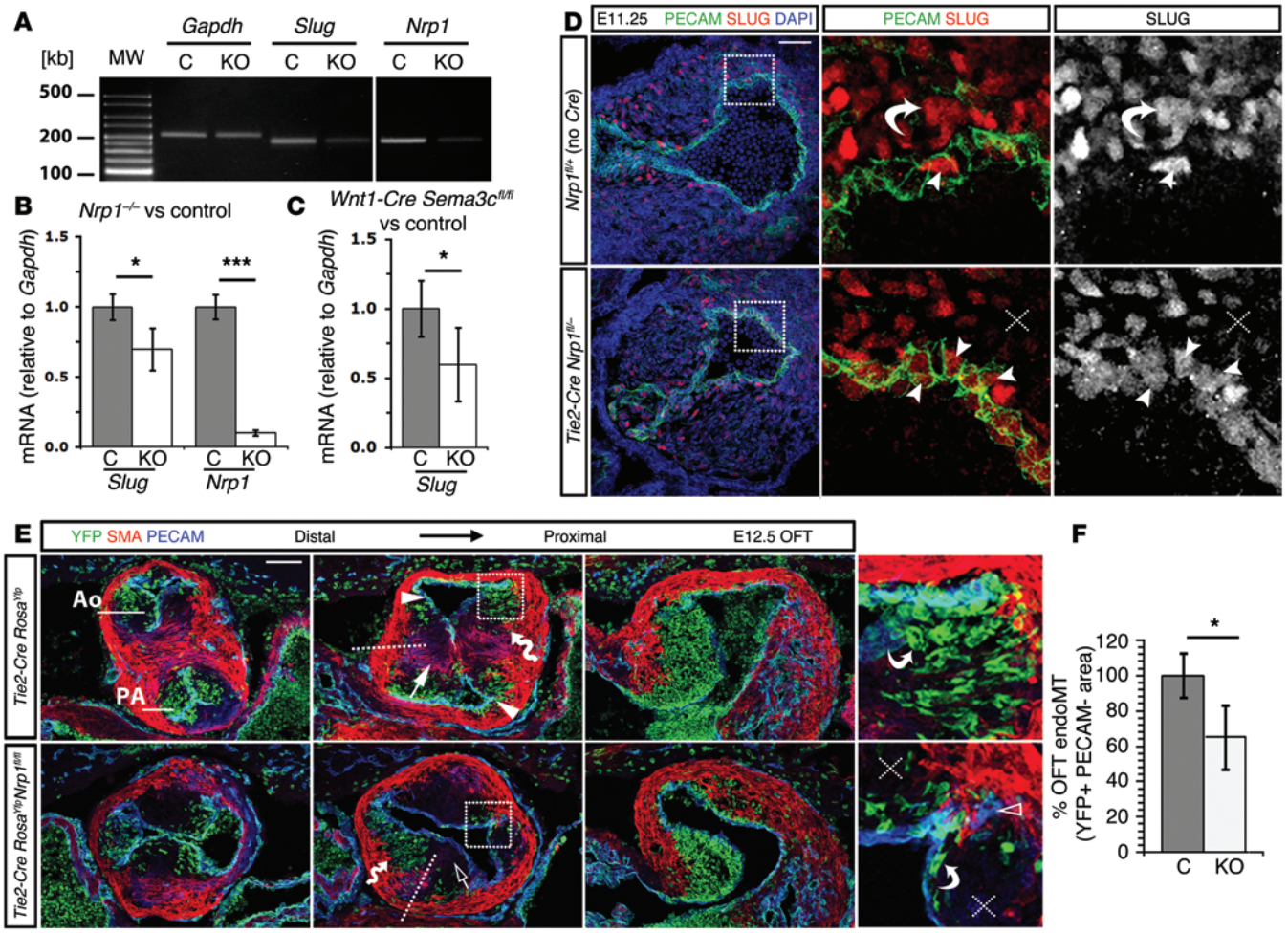

Figure 10. SEMA3C signaling through NRP1 induces endoMT in the OFT. (**A**–**C**) qRT-PCR of E10.5 OFT was used to evaluate *Nrp1*, *Slug*, and *Snail* expression relative to *Gapdh*, shown by gel electrophoresis (**A**) and qRT-PCR (**B** and **C**) of $Nrp1^{+/-}$ versus $Nrp1^{-/-}$ (n = 3 each) and $Sema3c^{fl/fl}$ (n = 3) versus *Wnt1-Cre* $Sema3c^{fl/fl}$ (n = 7). (**D**) Immunolabeling of OFT sections from E11.25 *Tie2-Cre* $Nrp1^{fl/-}$ and control OFTs (n = 3 each) for PECAM and SLUG; the single SLUG channel is shown in gray scale. The boxed area is shown at a higher magnification. Arrowheads indicate SLUG-expressing cells within the endothelium; the curved arrow indicates an example of a SLUG-expressing cell adjacent to the endothelium in the control, while the dotted cross indicates an area with few SLUG-positive cells in the mutant. (**E**) Serial sections of E12.5 OFTs from *Tie2-Cre* $Rosa^{Yfp}$ mice on a control $Nrp1^{fl/+}$ or mutant $Nrp1^{fl/fl}$ background at corresponding distal, medial, and proximal levels, immunolabeled for YFP, SMA, and PECAM. Solid arrowheads indicate endothelium; the solid arrow indicates septal bridge myocardialization; wavy arrows indicate migrating SMA-positive cells; and open arrows indicate absence of septal bridge formation. Dotted lines indicate the axis of septal bridge formation. Boxed areas are shown in higher magnification, with curved arrows highlighting cells that have undergone endoMT, dotted crosses showing areas lacking cells derived by endoMT, and the open arrowhead indicating an ectopic endothelial association with the myocardium. (**F**) Quantitation of YFP^+PECAM^- area in *Tie2-Cre* $Rosa^{Yfp}$ and *Tie2-Cre* $Rosa^{Yfp}$ $Nrp1^{fl/fl}$ E12.5 OFTs, n = 3 each. Mean ± SD. $^*P \le 0.05$; $^{***}P \le 0.001$, 2-tailed, unpaired Student's t test. Scale bars: 50 μm (**D**); 100 μm (**E**).

However, the importance of this pathway in vivo has so far only been demonstrated for arteriogenesis (57). In contrast, the results presented here show that mice lacking VEGF-A binding to NRP1 have normal OFT remodeling, even in the absence of NRP2. This finding was particularly unexpected because $Vegfa^{120/120}$ mice lacking the NRP1-binding VEGF164 isoform have defective OFT septation, although with only 50% penetrance (9). Our observations therefore imply that the phenotype of $Vegfa^{120/120}$ mice is not linked to NRP1's ability to bind VEGF-A. Instead, lack of extracellular matrix retention of VEGF120, known to be responsible for vascular-patterning defects in other tissues (58), may contribute to OFT defects in $Vegfa^{120/120}$ mice by reducing endothelial VEGFR2 signaling. Importantly, our results show that VEGF-A and SEMA3C are required for distinct aspects of OFT development.

Our finding that cardiac NCCs provide an essential source of *Sema3c* for OFT septation disagrees with the prior hypothesis that SEMA3C attracts NCCs into the OFT, but supports a role for SEMA3C as a signal secreted by NCCs. In agreement, the NCC-specific deletion of *Gata6*, which drives SEMA3C expression, also causes OFT defects (59). Even though SEMA3C was not required to attract cardiac NCCs into the OFT, and loss of SEMA3C receptors from cardiac NCCs did not impair OFT septation, these cells were indirectly affected by defective endothelial SEMA3C/NRP1 signaling. Thus, cardiac NCCs were abnormally placed in paired columns in the lateral parts of the endocardial cushions of E12.5 *Nrp1*-null mutants in positions where NCCs normally reside at earlier stages. Moreover, mutants lacking endothelial NRP1 or NCC-derived SEMA3C had similar defects. These observations suggest

that the convergence of the lateral NCC streams in the central OFT to enable septal bridge formation had failed in mutants with defective SEMA3C/NRP1 signaling in OFT endothelium and agree with the finding that NRP1-expressing primary ECs can respond to SEMA3C (60, 61). Moreover, it has been shown that SEMA3C binds to NRP1 in diverse cell types in vitro (24) and to NRP1-expressing vessels in vivo (62). Given that the only known SEMA3C receptors are NRP1 and NRP2, and in light of our expression studies, in vitro experiments, and genetic analyses, we conclude that NRP1 acts as an essential endothelial SEMA3C receptor during OFT septation, with a backup function for NRP2.

The incomplete penetrance of distal, as opposed to proximal, OFT septation defects in *Wnt1-Cre Sema3c*$^{fl/fl}$ and *Nrp1*$^{Sema/Sema}$ *Nrp2*$^{-/-}$ mice may be due to a number of factors. Variability in our analyses may be secondary to inefficient *Cre*-mediated targeting of the conditional *Sema3c*-null allele, whereas the *Nrp1*^{Sema} allele may encode a protein with residual ligand-binding activity. Additionally, incomplete penetrance may be secondary to stochastic or genetic background effects. In agreement, previous reports of constitutive *Sema3c*-null mutants described partially penetrant (75%) and partial (i.e., incomplete) OFT septation defects, with postnatal mortality of *Sema3c*-null mice being 50% lower on a C57BL/6 than on a CD1 background (8). Alternatively, *Nrp1*-null and *Tie2-Cre Nrp1*$^{fl/-}$ mutants with usually complete CAT may differ from *Nrp1*$^{Sema/Sema}$ *Nrp2*$^{-/-}$ mice with frequent partial CAT due to the existence of additional NRP1-dependent, but SEMA3C-independent pathways that contribute to OFT remodeling. Because *Nrp1*$^{Vegfa/Vegfa}$ mutants lacked OFT defects, an attractive possibility is a role for NRP1 in conveying signals provided by extracellular matrix molecules such as fibronectin, which can induce EC motility and cytoskeletal remodeling in an NRP1-dependent, but SEMA3- and VEGF-A–independent, pathway via the ABL1 and ABL2 kinases (63). In support of this idea, fibronectin is abundant in the remodeling OFT (64) and integrins have been implicated in OFT remodeling (26, 65).

Previous studies as well as our endothelial lineage tracing have shown that endoMT contributes significantly to endocardial cushion development in the proximal OFT (66). Moreover, mice with reduced BMP signaling have smaller endocardial cushions and lack proximal OFT septation (67), similar to *Wnt1-Cre Sema3c*$^{fl/fl}$ mutants. To address whether SEMA3C signaling through NRP1 promotes endoMT in the OFT, we used an explant assay that suggested that SEMA3C was sufficient to induce endoMT, that NCC-derived SEMA3C and NRP1 were both required for normal endoMT in this experimental setting, and that loss of endoMT in NRP1-deficient explants could not be rescued by exogenous SEMA3C. Furthermore, expression of *Slug*, a known marker of endoMT (42, 43), was reduced in the OFT of mice lacking SEMA3C or NRP1 compared with littermate controls just before the onset of endoMT. Finally, correlating with impaired *Slug* expression, mice lacking endothelial NRP1 showed a reduced contribution of endoMT-derived cells to the endocardial cushions of the proximal OFT. Interestingly, the enhanced expression of SEMA3C (68) or NRP1 (69) in cancer cells increases tumor invasiveness, a process in which tumor cells acquire mesenchymal properties analogous to endoMT. Thus, SEMA3C-dependent NRP1 signaling may represent a conserved mechanism that promotes the conversion of cells bound into noninvasive epithelial or endothelial monolayers into migratory single cells.

Some endoMT was still evident in the OFT of mice lacking SEMA3C signaling through NRP1, presumably because several complementary pathways contribute to this process. Thus, the SHF is a source for other molecules required for endoMT in the OFT, such as FGF8 (70, 71) and BMP4 (17, 72, 73). Furthermore, loss of Notch signaling in the SHF reduces FGF8 and BMP4 secretion, which is accompanied by impaired cardiac NCC immigration, reduced endoMT, and a failure of OFT septation (25). These prior studies concluded that SHF-derived mesoderm communicates with both cardiac NCCs and ECs to induce OFT septation. Our study has revealed an additional mechanism by which cardiac NCCs instruct the endothelium to help initiate endoMT and has also showed that endothelial signaling then instructs cardiac NCC relocalization for OFT septation. Accordingly, SEMA3C is one key member in a class of diverse molecules required for physiological endoMT during heart development. Further work will be necessary to determine how SEMA3C signaling through endothelial NRP1 interacts with or complements Notch, FGF8, and BMP4 signaling in the OFT. Interestingly, impaired cardiac NCC migration precedes defective endoMT observed within the OFT cushions of Notch, FGF8, and BMP4 mutants, reinforcing the idea that NCCs are causally linked to endoMT.

In summary, we have replaced prior hypotheses of NRP function in OFT remodeling with a substantially revised model, which embraces the complexity of developmental events that ensure proper OFT septation and involves multiple signaling events between the contributing cell lineages. Unraveling these complex interactions at the molecular and cellular level in mouse models will inform our interpretation of human genetic data obtained from patients with congenital heart defects, where a heterozygous single gene mutation is rarely found to be causative. In support of the idea that defective NRP1 signaling contributes to human congenital heart disease, a recent GWAS study uncovered a nucleotide polymorphism in the *NRP1* sequence that was associated with tetralogy of Fallot, while another study identified a homozygous splice mutation that ablates *NRP1* exon 3 in a patient with CAT and is predicted to disrupt the semaphorin-binding domain of *NRP1* (74, 75).

Methods

Mouse strains. Mice were paired in the evening, and the morning on which a vaginal plug was observed was defined as E0.5. Mice carrying *Nrp1*- or *Nrp2*-null alleles and *Vegfa*^{Lacz} reporter mice were maintained on a CD1 background (21, 76, 77). Mice carrying *Nrp1* alleles deficient in VEGF-A or semaphorin binding were maintained on a mixed SV126/C57BL/6 background (13, 23). Mice carrying conditional *Nrp1*-null (floxed) alleles (*Nrp1*$^{fl/fl}$) were mated to mice carrying the *Wnt1-Cre* (78) or *Tie2-Cre* (13, 79) transgenes and a heterozygous *Nrp1*-null allele and maintained on a C57BL/6 background (13, 79). The conditional *Sema3c*-null allele (*Sema3c*^{fl}) was generated through the Mouse Biology Program at UCD using a targeting vector from the Wellcome Trust Sanger Institute (project ID 69993, MGI:107557). Homologous recombination was performed in JM8A3.N1 embryonic stem cells, and positive clones were injected into C57BL/6 blastocysts. Chimeric mice were crossed to C57BL/6 mice to identify

germ-line transmission of the floxed allele. The selection cassette, flanked by 2 FRT sites, was removed by crossing *Sema3c*^{fl} mice to actin flippase mice (80). Conditional null mutants were generated by mating *Sema3c*$^{fl/fl}$ and *Wnt1-Cre Sema3c*$^{fl/+}$mice on a C57BL/6 background. Genotyping protocols are provided in Supplemental Table 1.

In situ hybridization, immunolabeling, and X-gal staining. Samples were fixed in 4% formaldehyde in PBS and processed as whole mounts or 20-μm cryosections. In situ hybridization (ISH) was performed with a digoxigenin-labeled riboprobe from a mouse *Sema3c* cDNA plasmid (gift of Jonathan Raper, University of Pennsylvania, Philadelphia, Pennsylvania, USA). Immunolabeling was carried out as described (81) using the following primary antibodies: rat anti-PECAM (553370, BD Biosciences – Pharmingen), rabbit anti-GFP (598, MBL), chick anti-GFP (GFP-1020, Aves), rabbit anti-SM22α (AB14106, Abcam), rabbit anti-SLUG (C19G7, Cell Signaling), rabbit anti-aCAS3 (9661, Cell Signaling), rabbit anti-pHH3 (06-570, Millipore), goat anti-NRP1, anti-VEGFR2, or anti-PLXNA2 (AF566, AF644 and AF5486, respectively, R&D Systems) as well as FITC- or Cy3-conjugated anti-SMA (F3777 and C6198, respectively, Sigma-Aldrich). Secondary antibodies used included Alexa Fluor–conjugated goat anti-rat, anti-chick, or anti-rabbit IgG (Life Technologies) and Cy3- or Alexa Fluor 647–conjugated rabbit anti-goat Fab fragment (Jackson ImmunoResearch). Nuclei were stained with DAPI (Life Technologies). Combined ISH and immunolabeling were carried out as previously described (82). β-Galactosidase activity from the *Lacz* transgene was visualized with X-gal (Sigma-Aldrich) (21). Samples were imaged with an MZ16 stereomicroscope (Leica) with Micropublisher camera (Perkin-Elmer) or an LSM710 laser-scanning confocal microscope (Zeiss). Images were processed with Adobe Photoshop CS4 (Adobe Inc.).

Ex vivo endoMT assay. For the endoMT assay (17), OFTs were dissected from E10.5 embryos and cultured with the OFT endothelium facing downwards in DMEM Glutamax supplemented with 10% FBS (Life Technologies) in a 24-well plate coated with 1 mg/ml collagen (BD Biosciences) at 37°C for 72 hours. Explants were fixed in 4% formaldehyde in PBS and stained with FITC-conjugated phalloidin (Sigma-Aldrich) and DAPI. Some explants were immunolabeled for YFP or PECAM. In some experiments, OFT explants were cultured in growth medium containing 1% serum and treated with 400 ng/ml mouse SEMA3C (R&D Systems).

RNA extraction and qRT-PCR. OFTs were dissected from E10.5 embryos, and total RNA was isolated using the RNeasy Micro Kit (QIAGEN). cDNA was synthesized by reverse transcription using Superscript III (Life Technologies). qRT-PCR was performed with 250 ng cDNA on an ABI 7500 Fast Real-Time PCR System (Applied Biosystems) using SYBR Green PCR Master Mix (Applied Biosystems) and 0.45 μg of the following oligonucleotides (Sigma-Aldrich): *Gapdh*, 5′-TGCGACTTCAACAGCAACTC-3′ and 5′-CTTGCTCAGTGTCCTTGCTG-3′, amplicon 200 bps; *Nrp1*, 5′- CCATTATAGACAGCACCATCC-3′ and 5′-AAGTTGCCATCTCCTGTATG-3′, amplicon 178 bps; *Slug*, 5′-TTCAACGCCTCCAAGAAGCC-3′ and 5′-GGGTAAAGGAGAGTGGAGTGG-3′, amplicon 183 bps; and *Sema3c* 5′-CCAGTGTGCACCTACCTGAA-3′ and 5′-TCGGGTTGAAAGAGCATCGT-3′ amplicon 103 bps. For each gene, the reaction was run in triplicate, and for each primer pair, a no-template control was included. Data were collected using Sequence Detector Software (SDS version 2.2; Applied Biosystems) and expression levels extrapolated using DART-PCR software (83) and normalized to *Gapdh* expression. In some experiments, qRT-PCR products were visualized by agarose (BDH Electran) gel electrophoresis.

Statistics. For each analysis, we examined at least 3 independent samples per experimental group; for qRT-PCR analysis, the average of triplicate reactions was used as the value of that sample. Results are expressed as mean ± SD relative to the specified controls. For all statistical analyses, we used a 2-tailed, unpaired Student's *t* test. *P* values of less than 0.05 were considered significant.

Study approval. Animal experiments were conducted with ethical approval from the Animal Welfare and Ethical Review Body of the UCL Institute of Ophthalmology and carried out under United Kingdom Home Office licence 70/7126.

Acknowledgments

We thank Catherine Roberts for helpful discussions and are grateful to Bertrand Vernay, Jenifer Suntharalingham, and Andy Joyce for technical help. We thank the staff of the Biological Resources Units at the UCL Institutes of Ophthalmology and Child Health for help with mouse husbandry and the Imaging Facility at the UCL Institute of Ophthalmology for the maintenance of the confocal microscope. This study was supported by a PhD studentship from the British Heart Foundation (FS/10/54/28680 to A. Plein), a Wellcome Trust New Investigator Award (095623/Z/11/Z to C. Ruhrberg), and a British Heart Foundation grant (RG/15/13/28570 to P.J. Scambler and A. Calmont).

Address correspondence to: Christiana Ruhrberg, UCL Institute of Ophthalmology, 11-43 Bath Street, London EC1V 9EL, United Kingdom. Phone: 4420.76084017; E-mail: c.ruhrberg@ucl.ac.uk. Or to: Peter Scambler, UCL Institute of Child Health, 30 Guilford Street, London WC1N 1EH, United Kingdom. Phone: 4420.79052635; E-mail: p.scambler@ucl.ac.uk.

1. Hoffman JI, Kaplan S. The incidence of congenital heart disease. *J Am Coll Cardiol*. 2002;39(12):1890–1900.
2. Williams JM, de Leeuw M, Black MD, Freedom RM, Williams WG, McCrindle BW. Factors associated with outcomes of persistent truncus arteriosus. *J Am Coll Cardiol*. 1999;34(2):545–553.
3. Markwald RR, Krook JM, Kitten GT, Runyan RB. Endocardial cushion tissue development: structural analyses on the attachment of extracellular matrix to migrating mesenchymal cell surfaces. *Scan Electron*. 1981;(pt 2):261–274.
4. Eisenberg LM, Markwald RR. Molecular regulation of atrioventricular valvuloseptal morphogenesis. *Circ Res*. 1995;77(1):1–6.
5. Sugishita Y, Watanabe M, Fisher SA. The development of the embryonic outflow tract provides novel insights into cardiac differentiation and remodeling. *Trends Cardiovasc Med*. 2004;14(6):235–241.
6. Kelly RG, Brown NA, Buckingham ME. The arterial pole of the mouse heart forms from Fgf10-expressing cells in pharyngeal mesoderm. *Dev Cell*. 2001;1(3):435–440.
7. van den Hoff MJ, et al. Myocardialization of the cardiac outflow tract. *Dev Biol*. 1999;212(2):477–490.
8. Feiner L, et al. Targeted disruption of semaphorin 3C leads to persistent truncus arteriosus and aortic arch interruption. *Development*. 2001;128(16):3061–3070.
9. Stalmans I, et al. VEGF: a modifier of the del22q11 (DiGeorge) syndrome? *Nat Med*. 2003;9(2):173–182.
10. Schwarz Q, Ruhrberg C. Neuropilin, you gotta let me know: should I stay or should I go? *Cell Adh*

Migr. 2010;4(1):61–66.
11. Kawasaki T, et al. A requirement for neuropilin-1 in embryonic vessel formation. *Development*. 1999;126(21):4895–4902.
12. Zhou J, Pashmforoush M, Sucov HM. Endothelial neuropilin disruption in mice causes DiGeorge syndrome-like malformations via mechanisms distinct to those caused by loss of Tbx1. *PLoS One*. 2012;7(3):e32429.
13. Gu C, et al. Neuropilin-1 conveys semaphorin and VEGF signaling during neural and cardiovascular development. *Dev Cell*. 2003;5(1):45–57.
14. Toyofuku T, et al. Repulsive and attractive semaphorins cooperate to direct the navigation of cardiac neural crest cells. *Dev Biol*. 2008;321(1):251–262.
15. Brown CB, et al. PlexinA2 and semaphorin signaling during cardiac neural crest development. *Development*. 2001;128(16):3071–3080.
16. Fantin A, et al. Tissue macrophages act as cellular chaperones for vascular anastomosis downstream of VEGF-mediated endothelial tip cell induction. *Blood*. 2010;116(5):829–840.
17. Bai Y, Wang J, Morikawa Y, Bonilla-Claudio M, Klysik E, Martin JF. Bmp signaling represses Vegfa to promote outflow tract cushion development. *Development*. 2013;140(16):3395–3402.
18. Ma HY, Xu J, Eng D, Gross MK, Kioussi C. Pitx2-mediated cardiac outflow tract remodeling. *Dev Dyn*. 2013;242(5):456–468.
19. Timmerman LA, et al. Notch promotes epithelial-mesenchymal transition during cardiac development and oncogenic transformation. *Genes Dev*. 2004;18(1):99–115.
20. Maden CH, Gomes J, Schwarz Q, Davidson K, Tinker A, Ruhrberg C. NRP1 and NRP2 cooperate to regulate gangliogenesis, axon guidance and target innervation in the sympathetic nervous system. *Dev Biol*. 2012;369(2):277–285.
21. Miquerol L, Gertsenstein M, Harpal K, Rossant J, Nagy A. Multiple developmental roles of VEGF suggested by a LacZ-tagged allele. *Dev Biol*. 1999;212(2):307–322.
22. Gerber HP, et al. VEGF is required for growth and survival in neonatal mice. *Development*. 1999;126(6):1149–1159.
23. Fantin A, et al. Neuropilin 1 (NRP1) hypomorphism combined with defective VEGF-A binding reveals novel roles for NRP1 in developmental and pathological angiogenesis. *Development*. 2014;141(3):556–562.
24. Gitler AD, Lu MM, Epstein JA. PlexinD1 and semaphorin signaling are required in endothelial cells for cardiovascular development. *Dev Cell*. 2004;7(1):107–116.
25. High FA, et al. Murine Jagged1/Notch signaling in the second heart field orchestrates Fgf8 expression and tissue-tissue interactions during outflow tract development. *J Clin Invest*. 2009;119(7):1986–1996.
26. Vallejo-Illarramendi A, Zang K, Reichardt LF. Focal adhesion kinase is required for neural crest cell morphogenesis during mouse cardiovascular development. *J Clin Invest*. 2009;119(8):2218–2230.
27. Chen H, He Z, Bagri A, Tessier-Lavigne M. Semaphorin-neuropilin interactions underlying sympathetic axon responses to class III semaphorins. *Neuron*. 1998;21(6):1283–1290.
28. Kaartinen V, Dudas M, Nagy A, Sridurongrit S, Lu MM, Epstein JA. Cardiac outflow tract defects in mice lacking ALK2 in neural crest cells. *Development*. 2004;131(14):3481–3490.
29. Wang J, Nagy A, Larsson J, Dudas M, Sucov HM, Kaartinen V. Defective ALK5 signaling in the neural crest leads to increased postmigratory neural crest cell apoptosis and severe outflow tract defects. *BMC Dev Biol*. 2006;6:51.
30. Kubalak SW, Hutson DR, Scott KK, Shannon RA. Elevated transforming growth factor beta2 enhances apoptosis and contributes to abnormal outflow tract and aortic sac development in retinoic X receptor alpha knockout embryos. *Development*. 2002;129(3):733–746.
31. Wang B, et al. Foxp1 regulates cardiac outflow tract, endocardial cushion morphogenesis and myocyte proliferation and maturation. *Development*. 2004;131(18):4477–4487.
32. Porter AG, Janicke RU. Emerging roles of caspase-3 in apoptosis. *Cell Death Differ*. 1999;6(2):99–104.
33. Sabine VS, Faratian D, Kirkegaard-Clausen T, Bartlett JM. Validation of activated caspase-3 antibody staining as a marker of apoptosis in breast cancer. *Histopathology*. 2012;60(2):369–371.
34. Sharma PR, Anderson RH, Copp AJ, Henderson DJ. Spatiotemporal analysis of programmed cell death during mouse cardiac septation. *Anat Rec A Discov Mol Cell Evol Biol*. 2004;277(2):355–369.
35. Barbosky L, et al. Apoptosis in the developing mouse heart. *Dev Dyn*. 2006;235(9):2592–2602.
36. Nomura-Kitabayashi A, et al. Outflow tract cushions perform a critical valve-like function in the early embryonic heart requiring BMPRIA-mediated signaling in cardiac neural crest. *Am J Physiol Heart Circ Physiol*. 2009;297(5):H1617–H1628.
37. Hendzel MJ, et al. Mitosis-specific phosphorylation of histone H3 initiates primarily within pericentromeric heterochromatin during G2 and spreads in an ordered fashion coincident with mitotic chromosome condensation. *Chromosoma*. 1997;106(6):348–360.
38. Tapia C, Kutzner H, Mentzel T, Savic S, Baumhoer D, Glatz K. Two mitosis-specific antibodies, MPM-2 and phospho-histone H3 (Ser28), allow rapid and precise determination of mitotic activity. *Am J Surg Pathol*. 2006;30(1):83–89.
39. Jiang X, Rowitch DH, Soriano P, McMahon AP, Sucov HM. Fate of the mammalian cardiac neural crest. *Development*. 2000;127(8):1607–1616.
40. Flagg AE, Earley JU, Svensson EC. FOG-2 attenuates endothelial-to-mesenchymal transformation in the endocardial cushions of the developing heart. *Dev Biol*. 2007;304(1):308–316.
41. Nakajima Y, Morishima M, Nakazawa M, Momma K. Inhibition of outflow cushion mesenchyme formation in retinoic acid-induced complete transposition of the great arteries. *Cardiovasc Res*. 1996;31(spec no):E77–E85.
42. Niessen K, Fu Y, Chang L, Hoodless PA, McFadden D, Karsan A. Slug is a direct Notch target required for initiation of cardiac cushion cellularization. *J Cell Biol*. 2008;182(2):315–325.
43. Leong KG, et al. Jagged1-mediated Notch activation induces epithelial-to-mesenchymal transition through Slug-induced repression of E-cadherin. *J Exp Med*. 2007;204(12):2935–2948.
44. Nagaishi M, Nobusawa S, Tanaka Y, Ikota H, Yokoo H, Nakazato Y. Slug, twist, and E-cadherin as immunohistochemical biomarkers in meningeal tumors. *PLoS One*. 2012;7(9):e46053.
45. Mikami S, et al. Expression of Snail and Slug in renal cell carcinoma: E-cadherin repressor Snail is associated with cancer invasion and prognosis. *Lab Invest*. 2011;91(10):1443–1458.
46. Hotz B, Arndt M, Dullat S, Bhargava S, Buhr HJ, Hotz HG. Epithelial to mesenchymal transition: expression of the regulators snail, slug, and twist in pancreatic cancer. *Clin Cancer Res*. 2007;13(16):4769–4776.
47. Kim JY, Kim YM, Yang CH, Cho SK, Lee JW, Cho M. Functional regulation of Slug/Snail2 is dependent on GSK-3beta-mediated phosphorylation. *FEBS J*. 2012;279(16):2929–2939.
48. Chen H, Chedotal A, He Z, Goodman CS, Tessier-Lavigne M. Neuropilin-2, a novel member of the neuropilin family, is a high affinity receptor for the semaphorins Sema E and Sema IV but not Sema III. *Neuron*. 1997;19(3):547–559.
49. Escot S, Blavet C, Hartle S, Duband JL, Fournier-Thibault C. Misregulation of SDF1-CXCR4 signaling impairs early cardiac neural crest cell migration leading to conotruncal defects. *Circ Res*. 2013;113(5):505–516.
50. Tachibana K, et al. The chemokine receptor CXCR4 is essential for vascularization of the gastrointestinal tract. *Nature*. 1998;393(6685):591–594.
51. Nagasawa T, et al. Defects of B-cell lymphopoiesis and bone-marrow myelopoiesis in mice lacking the CXC chemokine PBSF/SDF-1. *Nature*. 1996;382(6592):635–638.
52. Takahashi T, Nakamura F, Jin Z, Kalb RG, Strittmatter SM. Semaphorins A and E act as antagonists of neuropilin-1 and agonists of neuropilin-2 receptors. *Nat Neurosci*. 1998;1(6):487–493.
53. Chen H, et al. Neuropilin-2 regulates the development of selective cranial and sensory nerves and hippocampal mossy fiber projections. *Neuron*. 2000;25(1):43–56.
54. Fantin A, Schwarz Q, Davidson K, Normando EM, Denti L, Ruhrberg C. The cytoplasmic domain of neuropilin 1 is dispensable for angiogenesis, but promotes the spatial separation of retinal arteries and veins. *Development*. 2011;138(19):4185–4191.
55. Zhang Y, et al. Tie2Cre-mediated inactivation of plexinD1 results in congenital heart, vascular and skeletal defects. *Dev Biol*. 2009;325(1):82–93.
56. Soker S, Miao HQ, Nomi M, Takashima S, Klagsbrun M. VEGF165 mediates formation of complexes containing VEGFR-2 and neuropilin-1 that enhance VEGF165-receptor binding. *J Cell Biochem*. 2002;85(2):357–368.
57. Lanahan A, et al. The neuropilin 1 cytoplasmic domain is required for VEGF-A-dependent arteriogenesis. *Dev Cell*. 2013;25(2):156–168.
58. Ruhrberg C, et al. Spatially restricted patterning cues provided by heparin-binding VEGF-A control blood vessel branching morphogenesis. *Genes Dev*. 2002;16(20):2684–2698.
59. Lepore JJ, Mericko PA, Cheng L, Lu MM, Morrisey EE, Parmacek MS. GATA-6 regulates semaphorin 3C and is required in cardiac neural crest for cardiovascular morphogenesis. *J Clin Invest*.

2006;116(4):929–939.
60. Banu N, Teichman J, Dunlap-Brown M, Villegas G, Tufro A. Semaphorin 3C regulates endothelial cell function by increasing integrin activity. *FASEB J*. 2006;20(12):2150–2152.
61. Salikhova A, et al. Vascular endothelial growth factor and semaphorin induce neuropilin-1 endocytosis via separate pathways. *Circ Res*. 2008;103(6):e71–e79.
62. Vieira JM, Schwarz Q, Ruhrberg C. Role of the neuropilin ligands VEGF164 and SEMA3A in neuronal and vascular patterning in the mouse. *Novartis Found Symp*. 2007;283:230–235.
63. Raimondi C, Fantin A, Lampropoulou A, Denti L, Chikh A, Ruhrberg C. Imatinib inhibits VEGF-independent angiogenesis by targeting neuropilin 1-dependent ABL1 activation in endothelial cells. *J Exp Med*. 2014;211(6):1167–1183.
64. Burke RD, Wang D, Jones VM. Ontogeny of vessel wall components in the outflow tract of the chick. *Anat Embryol (Berl)*. 1994;189(5):447–456.
65. Dai X, et al. Requirement for integrin-linked kinase in neural crest migration and differentiation and outflow tract morphogenesis. *BMC Biol*. 2013;11:107.
66. Person AD, Klewer SE, Runyan RB. Cell biology of cardiac cushion development. *Int Rev Cytol*. 2005;243:287–335.
67. Delot EC, Bahamonde ME, Zhao M, Lyons KM. BMP signaling is required for septation of the outflow tract of the mammalian heart. *Development*. 2003;130(1):209–220.
68. Herman JG, Meadows GG. Increased class 3 semaphorin expression modulates the invasive and adhesive properties of prostate cancer cells. *Int J Oncol*. 2007;30(5):1231–1238.
69. Peng Y, Liu YM, Li LC, Wang LL, Wu XL. MicroRNA-338 inhibits growth, invasion and metastasis of gastric cancer by targeting NRP1 expression. *PLoS One*. 2014;9(4):e94422.
70. Frank DU, et al. An Fgf8 mouse mutant phenocopies human 22q11 deletion syndrome. *Development*. 2002;129(19):4591–4603.
71. Park EJ, et al. Required, tissue-specific roles for Fgf8 in outflow tract formation and remodeling. *Development*. 2006;133(12):2419–2433.
72. McCulley DJ, Kang JO, Martin JF, Black BL. BMP4 is required in the anterior heart field and its derivatives for endocardial cushion remodeling, outflow tract septation, and semilunar valve development. *Dev Dyn*. 2008;237(11):3200–3209.
73. Liu W, et al. Bmp4 signaling is required for outflow-tract septation and branchial-arch artery remodeling. *Proc Natl Acad Sci U S A*. 2004;101(13):4489–4494.
74. Cordell HJ, et al. Genome-wide association study identifies loci on 12q24 and 13q32 associated with tetralogy of Fallot. *Hum Mol Genet*. 2013;22(7):1473–1481.
75. Shaheen R, et al. Positional mapping of PRKD1, NRP1 and PRDM1 as novel candidate disease genes in truncus arteriosus. *J Med Genet*. 2015;52(5):322–329.
76. Giger RJ, Urquhart ER, Gillespie SK, Levengood DV, Ginty DD, Kolodkin AL. Neuropilin-2 is a receptor for semaphorin IV: insight into the structural basis of receptor function and specificity. *Neuron*. 1998;21(5):1079–1092.
77. Kitsukawa T, et al. Neuropilin-semaphorin III/D-mediated chemorepulsive signals play a crucial role in peripheral nerve projection in mice. *Neuron*. 1997;19(5):995–1005.
78. Schwarz Q, Maden CH, Vieira JM, Ruhrberg C. Neuropilin 1 signaling guides neural crest cells to coordinate pathway choice with cell specification. *Proc Natl Acad Sci U S A*. 2009;106(15):6164–6169.
79. Fantin A, et al. NRP1 acts cell autonomously in endothelium to promote tip cell function during sprouting angiogenesis. *Blood*. 2013;121(12):2352–2362.
80. Rodriguez CI, et al. High-efficiency deleter mice show that FLPe is an alternative to Cre-loxP. *Nat Genet*. 2000;25(2):139–140.
81. Vieira JM, Schwarz Q, Ruhrberg C. Selective requirements for NRP1 ligands during neurovascular patterning. *Development*. 2007;134(10):1833–1843.
82. Antypa M, Faux C, Eichele G, Parnavelas JG, Andrews WD. Differential gene expression in migratory streams of cortical interneurons. *Eur J Neurosci*. 2011;34(10):1584–1594.
83. Peirson SN, Butler JN, Foster RG. Experimental validation of novel and conventional approaches to quantitative real-time PCR data analysis. *Nucleic Acids Res*. 2003;31(14):e73.